JOC The Journal of Organic Chemistry

Article

pubs.acs.org/joc

Quantitative Assessment of Aromaticity and Antiaromaticity Utilizing Vibrational Spectroscopy

Dani Setiawan, Elfi Kraka, and Dieter Cremer*

Computational and Theoretical Chemistry Group (CATCO), Department of Chemistry, Southern Methodist University, 3215 Daniel Ave., Dallas, Texas 75275-0314, United States

Supporting Information

ABSTRACT: Vibrational frequencies can be measured and calculated with high precision. Therefore, they are excellent tools for analyzing the electronic structure of a molecule. In this connection, the properties of the local vibrational modes of a molecule are best suited. A new procedure is described, which utilizes local CC stretching force constants to derive an aromaticity index (AI) that quantitatively determines the degree of π-delocalization in a cyclic conjugated system. Using Kekulé benzene as a suitable reference, the AIs of 30 mono- and polycyclic conjugated hydrocarbons are calculated. The AI turns out to describe π-delocalization in a balanced way by correctly describing local aromatic units, peripheral, and all-bond delocalization. When comparing the AI with the harmonic oscillator model of AI, the latter is found to exaggerate the antiaromaticity of true and potential $4n$ π-systems or to wrongly describe local aromaticity. This is a result of a failure of the Badger relationship (the shorter bond is always the stronger bond), which is only a rule and therefore cannot be expected to lead to an accurate description of the bond strength via the bond length. The AI confirms Clar's rule of disjoint benzene units in many cases, but corrects it in those cases where peripheral π-delocalization leads to higher stability. [5]-, [6]-, [7]-Circulene and Kekulene are found to be aromatic systems with varying degree of delocalization. Properties of the local vibrational modes provide an accurate description of π-delocalization and an accurate AI.

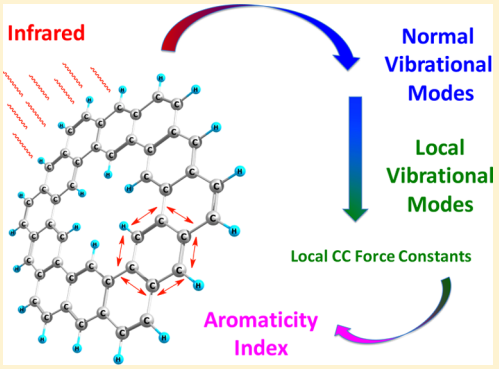

1. INTRODUCTION

Aromaticity and antiaromaticity are important concepts in chemistry as they help to explain physical and chemical properties of cyclic π-conjugated compounds.[1−8] Essential to these concepts are Hückel's $4n + 2$ and $4n$ π-electron rules,[9,10] which associate a simple count of π-electrons with the stability and reactivity of the π-system in question. During the last 80 years since the formulation of the Hückel rules, the concepts of aromaticity and antiaromaticity have been probed with regard to almost every molecular property. A multitude of methods and procedures has been developed to define and measure the degree of aromaticity in polyaromatic hydrocarbons (PAHs), their heteroatomic analogues,[11−18] to estimate the influence of substituent effects on aromaticity,[19−24] and to determine the degree of aromaticity in nonplanar compounds.[25−30] The performance of the different approaches has been tested and compared.[31−33]

Hückel's original description of aromaticity was based on the *topology* (see Figure 1) of the net of π-bonds in a molecule and is the basis of molecular orbital (MO) descriptions of (anti)aromatic systems.[34,35] Clar's sextet rule[36] is another example for the simple use of the topological features of a π-system. It requires a maximum number of disjoint aromatic benzene units and a minimum number of localized double bonds in a benzenoide hydrocarbon and has provided astonishingly reliable predictions as to the preferred delocalization pattern of PAHs.[37−40] Other topological descriptions use double-bond equivalents (DBEs),[41] chemical graph theory (CGT),[42−45] multicenter indices such as the ring center index I_{ring},[46] the multicenter index MCI,[31,47−49] or the electron localization−delocalization matrix (LDM).[50,51]

More advanced approaches have used *thermochemical properties* (Figure 1) such as the molecular energy (enthalpy) to define a resonance or aromatic stabilization (aromatization) energy ASE and relating this energy to the thermodynamic stability of a conjugated system.[52−57] Similarly, the topological resonance energy (TREs),[44] the bond resonance energy (BRE),[53,58] the superaromatic stabilization energy (SSE),[56] the energy decomposition analysis,[54] or bond centered group additivity schemes[59] have been used to quantify the effects of π-delocalization.

Alternatively, one can use the *molecular geometry* (Figure 1) to determine the degree of bond equilibration under the impact of π-delocalization.[11,75,76] Especially popular were the harmonic oscillator model HOMA,[60] the reformulated HOMA (rHOMA),[61,62] the electron delocalization-based HOMA (HOMED),[63] its extension HOMHED for heteroatoms,[64] and the various applications of the HOMA approaches.[30,77−80] Of course, bond lengths always depend on strain, exchange

Received: July 22, 2016
Published: September 16, 2016

DOI: 10.1021/acs.joc.6b01761
J. Org. Chem. 2016, 81, 9669−9686

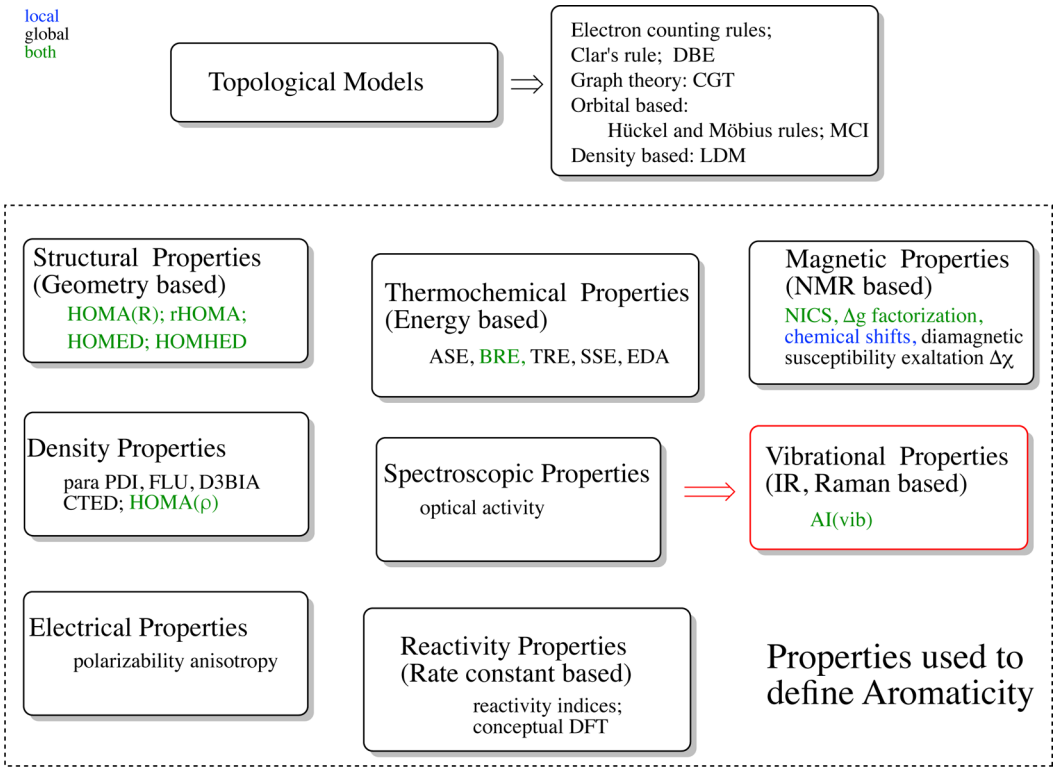

Figure 1. Overview over the various (anti)aromaticity descriptors used: DBE, double bond equivalent;[41] CGT, chemical graph theory;[42−45] MCI, multicenter index;[31,47−49] LDM, electron localization−delocalization matrix;[50,51] HOMA(R), original harmonic oscillator model of aromaticity based on bond lengths *R*;[60] rHOMA, reformulated HOMA;[61,62] HOMED, electron delocalization-based HOMA,[63] HOMHED, HOMED for heteroatoms;[64] ASE, aromatic stabilization energy;[57,65] BRE, bond resonance energy;[53,58] TRE, topological resonance energy;[44] SSE, superaromatic stabilization energy;[56] EDA, energy decomposition analysis;[54] NICS, nucleus-independent chemical shift;[22,25,66,67] Δ*g*, average gyromagnetic factor;[68] p-PDI, para-delocalization index;[69] FLU, aromatic fluctuation index;[70] D3BIA, density and degeneracy-based index of aromaticity;[71] CTED, corrected total electron density;[72] HOMA(ρ), HOMA based on the electron density ρ at the bond critical point;[73,74] AI(vib), aromaticity index based on the molecular vibrations.

repulsion, core polarization, and other effects and often fail to function as reliable bond strength and/or delocalization parameters.[81−85] Therefore, HOMA indices should always be compared with other measures of electron delocalization.

The *magnetic properties*(Figure 1) of (anti)aromatic molecule are better suited to describe delocalization phenomena, e.g., with the help of the diamagnetic susceptibility exaltation $\Delta\chi$,[86] the NMR chemical shifts, their nucleus-independent analogues NICS (nucleus-independent chemical shift),[22,25,66,67] diatropic and paratropic ring currents,[1,87,88] the polygonal current model,[24] or the average *g*-factor of a hydrogen atom placed above a π-system as suitable magnetic probe.[68] One could argue that the magnetic properties of a molecule are sufficiently detailed and so sensitive that any (anti)aromatic delocalization can be directly detected. However, magnetic properties are also affected by local anisotropies and can reflect σ−, and core-contributions, which one actually wants to separate from the π-delocalization effects. It is well-known that the NICS values exaggerate the aromatic character of large ring systems and have problem transition-metal clusters/complexes[89] and that indirect spin−spin coupling constants $J(^{13}C^{13}C)$ only provide reliable measures of π-delocalization in some well-defined cases.[90−92]

If π-delocalization dominates the electronic structure, the *electron density distribution* (Figure 1) can be used to develop indicators for (anti)aromaticity, as has been amply done within the framework of Bader's virial partitioning analysis.[93] The derivation of bond orders and π-ellipticities for cyclic π-systems has to be mentioned in this connection.[94−97] More recently, one has developed delocalization indices such as the para-delocalization index (PDI),[69] the source function,[98] the aromatic fluctuation index (FLU),[70] the corrected total electron density (CTED) index,[72] the density- and degeneracy-based index of aromaticity (D3BIA),[71] the anisotropy of the π-electron density distribution,[99] or the analysis of the electron density in terms of electron localization and delocalization.[100] In addition, one has extended the HOMA approach to the electron density in form of HOMA(ρ_b) by replacing distance *R* by the electron density at the bond critical point.[73,74]

Although electron density-based delocalization descriptors have added to the understanding of (anti)aromaticity, a simple measure of the intrinsic bond strength, which can be used to quantify the degree of π-delocalization, is difficult to obtain from the local electron density properties without considering the electron distribution in the total bond region. Cremer and Gauss[101] have shown that the covalent part of the intrinsic strength of a bond can only be obtained by integrating over the electron density in the zero-flux surface between two bonded atoms. These authors also pointed out that only by simultaneously evaluating the ionic (polar) part of the intrinsic bond strength, a reasonable account of the bond strength can be given. This clearly shows that it is not possible to obtain exact information about the intrinsic bond strength and π-delocalization by determining the electron density at singular points. Similar considerations apply to other parameters such as the electron localization function (ELF),[102] the generalized

DOI: 10.1021/acs.joc.6b01761
J. Org. Chem. 2016, 81, 9669−9686

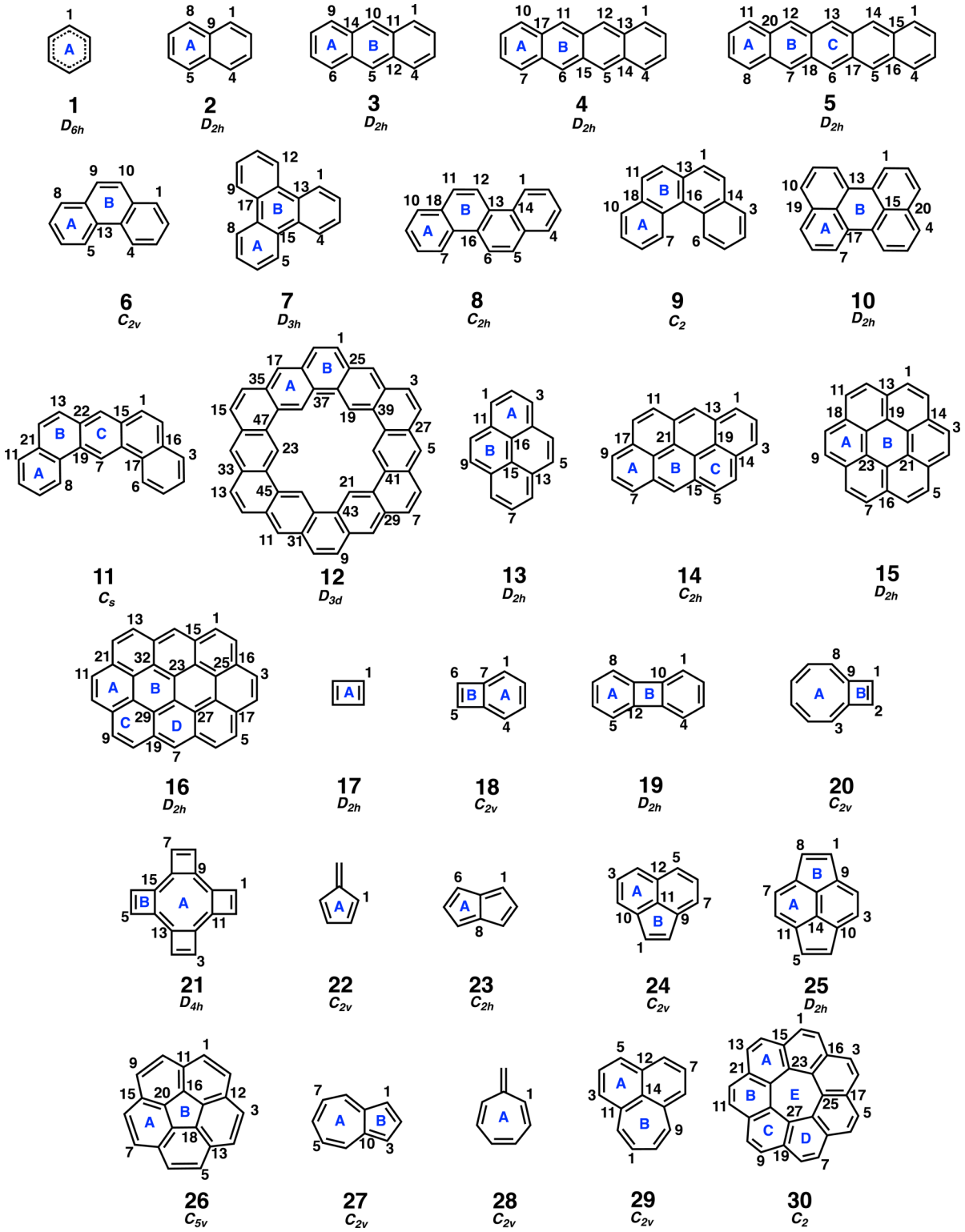

Figure 2. Cyclic and polycyclic hydrocarbons investigated in this study. Small numbers indicate the numbering of carbon atoms used in this work. Individual rings are indicated by blue letters A, B, etc.

Polanski index,[103] the DFT linear response as a measure for aromaticity,[104] or the anisotropy of the current-induced density (ACID).[105]

There have been scattered attempts to use *electrical properties* such as the molecular dipole polarizability[104,106,107] to describe (anti)aromaticity. The connection between aromaticity and reactivity has been investigated,[7,108,109] and reactions with aromatic transition states have been studied.[110,111] Also little use has been made to use *spectroscopic properties* (Figure 1) to describe aromaticity.[112−114] Molecular spectroscopy offers a variety of tools for the evaluation of aromaticity in the whole molecule or parts thereof by measuring physicochemical properties that reflect a manifestation of its aromatic character.[115,116] A spectroscopic tool as sensitive as NMR

DOI: 10.1021/acs.joc.6b01761
J. Org. Chem. 2016, 81, 9669−9686

spectroscopy is vibrational spectroscopy. The molecular vibrations probe each part of the electronic structure of a molecule, and therefore, it should be possible to derive a sensitive descriptor of π-electron delocalization utilizing measured and/or computed vibrational properties (red box in Figure 1). Recently, we have started to derive delocalization indices directly from measured vibrational frequencies.[117] Since the number of cyclic π-stems with a complete set of measured vibrational frequencies is rather limited,[118,119] the description of (anti)aromatic molecules with the help of measured vibrational frequencies was more a proof of concept than to determine the full power of this approach.[117] The latter is at the focus of the current work and for that purpose, vibrational frequencies will be determined with a suitable quantum chemical method.

The use of vibrational frequencies to describe π-delocalization implies four steps: (1) Conversion of frequency data to force constants because only the latter are mass-independent and therefore directly reflect the electronic structure of a molecule; (2) kinematic decoupling of the normal vibrational modes and obtaining local mode stretching force constants, which describe the intrinsic strength of a given bond; (3) introduction of suitable reference molecules to convert local stretching force constants to relative bond strength orders (BSOs); and (4) use of an aromaticity model to derive from BSO values a suitable vibrational aromaticity index AI(vib) (in short: AI) that quantitatively assesses the degree of π-delocalization. By means of this four-step approach, we will answer a number of pending questions: (1) What are the (dis)advantages and the limitations of using vibrational properties as descriptors for (anti)aromaticity? (2) How important is the choice of a suitable reference for quantitatively determining the degree of π-delocalization? Is there a general way to select suitable reference systems so that the AI can be applied as frequent as in the case of other model-based approaches? (3) Can one distinguish between local, peripheral, and global (anti)aromaticity? What is the preferred delocalization mode for a given π-system? (4) Are there situations in which the topology of a conjugated ring system enforces antiaromatic character, or is there always a global nonaromatic or aromatic alternative to local antiaromaticity? (5) To which extend are simple, model-based predictions such as Clar's rule applicable and justified? (6) Are there any π-systems that have been described in an erroneous way by other approaches, which can now be corrected due to the higher sensitivity and reliability of vibrational spectroscopy?

The answers to these questions will be presented in the following way. In Section 2, details of the computational methods used in the current investigation will be presented. In Section 3, the AI derived in this work will be applied to the 30 molecules shown in Figure 2, and results will be discussed with regard to the questions posted above. Finally in Section 4, the conclusions of this work will be summarized.

2. COMPUTATIONAL METHODS

The current work is based on the properties of the local vibrational modes of a molecule as originally derived by Konkoli and Cremer.[120] The normal vibrational modes of a molecule are always delocalized because of electronic and kinematic (mass) mode−mode coupling.[81,121−123] Electronic coupling is suppressed by solving the Wilson equation, which is based on the Euler−Lagrange equations.[121] Konkoli and Cremer[120] derived mass-decoupled Euler−Lagrange equations and suppressed in this way also the kinematic coupling between the vibrational modes. By solving the mass-decoupled analogue of the Wilson equation, local vibrational modes are obtained. The local modes are unique and the local counterparts of the normal vibrational modes.[124,125] Any internal coordinate can drive a local mode (*leading parameter principle*,[120] where however only those local modes, which are connected to the normal modes in an adiabatic connection scheme[124,125] constitute the unique set of $3N - L$ local modes (N: number of atoms in a molecule; L: number of translations and rotations).

The computational details of how to obtain the local mode properties from normal mode data have been described elsewhere.[120,126] To obtain the degree of π-delocalization, the local CC stretching force constants k^a(CC) have been calculated for molecules **1**−**30** shown in Figure 2. The local stretching force constant probes the strength of a bond for an infinitesimal change in the atomic positions. Recently, Zou and Cremer have shown that the intrinsic dissociation energy of a specific bond is linearly related to its local stretching force constant.[127] Hence, k^a(CC) is a direct measure of the intrinsic strength of the CC bond and by this reflects its properties as a result of π-delocalization.

For the purpose of simplifying a comparison of stretching force constants, a relative bond strength order (BSO) n(CC) has been derived. For this purpose, the CC single bond in ethane (n = 1.000) and the CC double bond in ethene (n = 2.000) were chosen as suitable references. By applying the extended Badger rule,[123,128,129] one can show that the BSO is related to the local stretching force constant by a power relationship, which is fully determined by the two reference values and the requirement that for a zero-force constant, the BSO value must also be zero. In this way, the relationship BSO(CC) = $a(k^a)^b$, where a(CC) and b(CC) are 0.329 and 0.796, was obtained.

In a somewhat different way, a relative BSO for CH bonds was derived. Since it is difficult to define a CH bond with a specific fractional BSO value, the FH bond was used instead. The $D_{\infty h}$-symmetrical complex $[F\cdots H\cdots F]^-$ is an example for a system with a covalent H-bond with bond order n(FH) = 0.500. By determining the local F,H stretching force constants for FH (n(FH) = 1.000) and $[F\cdots H\cdots F]^-$ and enforcing $n(FH) = 0$ for $k^a = 0$, a second power relationship was obtained with a = 0.493 and b = 0.315. With this relationship, the BSO(CH) value of methane is 0.832. By shifting all BSO(CH) values by 0.168 according to BSO(CC) = $a(k^a)^b + c$ (c = 0.168), all CH bonds investigated in this work are referenced with regard to BSO(CH, methane) = 1.000.

A suitable AI was derived by utilizing HOMA, which takes for benzenoide hydrocarbons Kekulé benzene as a reference, assuming that no π-delocalization effects are encountered other than those in an acyclic polyene.[60,61,75,130] The HOMA index can be detailed by determining the optimal CC bond length R_{opt} of the reference molecule and the average CC bond length of the target molecule so that eq 1 can be split into two parts (see eq 2), where the first measures bond weakening/strengthening (EN) and the second bond alternation (GEO) (see eq 3):[60,61,75,130]

$$\mathrm{HOMA} = 1 - \frac{\alpha}{\mathrm{NB}} \sum (R_{opt} - R_i)^2 \quad (1)$$

$$\mathrm{HOMA} = 1 - \alpha\left[(R_{opt} - R_{av})^2 + \frac{1}{\mathrm{NB}} \sum (R_{av} - R_i)^2\right] \quad (2)$$

$$\mathrm{HOMA} = 1 - \mathrm{EN} - \mathrm{GEO} \quad (3)$$

where R_{opt} given in Å is determined by averaging the single- and double-bond lengths of Kekulé benzene, which are modeled by the CC bonds of *trans*-1,3-butadiene.[117] The constant α (in Å^{-2}) is used to enforce a HOMA value of zero for Kekulé benzene. In the present work, R_{opt} and α take values of 1.393 and 282.94 Å^{-2}. NB is the number of CC bonds in the targeted π-system. R_i denotes an individual bond length in the molecule under consideration.[130]

Although the HOMA index based on bond lengths R_i has been amply used,[60,61,75,130] the bond length R is often a problematic bond strength descriptor, as has been pointed out by several authors.[76,81] Andrzejak and co-workers[76] have shown that HOMA indices determined with eq 1 strongly depend on the way Kekulé benzene as the reference without aromatic π-delocalization is modeled and the

DOI: 10.1021/acs.joc.6b01761
J. Org. Chem. 2016, 81, 9669−9686

Table 1. AI and HOMA Indices for Molecules 1−30

				anharmonic			harmonic					
no.	molecule	formula	R	AI	WS	ALT	AI	WS	ALT	HOMA	EN	GEO
31	Kekulé benzene	C_6H_6	O	0.000	0.000	1.000	0.000	0.000	1.000	0.000	0.000	1.000
1	benzene	C_6H_6	P	0.924	0.076	0.000	0.926	0.074	0.000	0.998	0.002	0.000
2	naphtalene	$C_{10}H_8$	P	0.773	0.106	0.121	0.775	0.104	0.121	0.862	0.004	0.134
			O	0.744	0.132	0.124	0.748	0.129	0.123	0.844	0.012	0.145
			A	0.721	0.155	0.124	0.726	0.151	0.123	0.828	0.022	0.150
3	anthracene	$C_{14}H_{10}$	P	0.722	0.116	0.162	0.725	0.112	0.163	0.811	0.007	0.181
			O	0.665	0.164	0.171	0.668	0.160	0.172	0.759	0.030	0.211
			A	0.591	0.183	0.226	0.595	0.177	0.228	0.679	0.049	0.273
			B	0.678	0.262	0.060	0.683	0.257	0.060	0.797	0.077	0.126
4	tetracene	$C_{18}H_{12}$	P	0.701	0.131	0.168	0.712	0.118	0.170	0.801	0.009	0.190
			O	0.616	0.199	0.185	0.630	0.183	0.187	0.713	0.044	0.243
			A	0.509	0.204	0.287	0.519	0.190	0.291	0.582	0.068	0.350
			B	0.594	0.320	0.086	0.620	0.294	0.086	0.712	0.109	0.179
5	pentacene	$C_{22}H_{14}$	P				0.656	0.152	0.192	0.728	0.026	0.246
			O				0.610	0.202	0.188	0.694	0.054	0.252
			A				0.477	0.197	0.326	0.537	0.080	0.383
			B				0.571	0.314	0.115	0.650	0.129	0.221
			C				0.589	0.339	0.072	0.673	0.137	0.190
6	phenanthrene	$C_{14}H_{10}$	P	0.715	0.137	0.148	0.718	0.132	0.149	0.790	0.016	0.194
			O	0.697	0.165	0.138	0.702	0.159	0.139	0.789	0.029	0.182
			A	0.788	0.143	0.069	0.795	0.136	0.069	0.906	0.009	0.085
			B	0.472	0.295	0.233	0.477	0.292	0.231	0.552	0.176	0.272
7	triphenylene	$C_{18}H_{12}$	P	0.666	0.221	0.112	0.707	0.176	0.117	0.728	0.037	0.235
			O	0.555	0.363	0.082	0.707	0.191	0.102	0.747	0.047	0.205
			A	0.781	0.159	0.060	0.824	0.118	0.058	0.931	0.004	0.065
			B	0.344	0.607	0.049	0.354	0.595	0.051	0.255	0.586	0.160
8	[2H_{12}]chrysene	$C_{18}H_{12}$	P	0.669	0.156	0.175	0.671	0.154	0.175	0.757	0.028	0.215
			O	0.664	0.180	0.156	0.667	0.177	0.156	0.765	0.041	0.194
			A	0.773	0.142	0.085	0.777	0.138	0.085	0.886	0.011	0.104
			B	0.571	0.250	0.179	0.550	0.265	0.185	0.656	0.129	0.215
9	benzo[*c*]phenanthrene	$C_{18}H_{12}$	P				0.628	0.178	0.194	0.743	0.033	0.225
			O	0.779	0.065	0.157	0.607	0.207	0.186	0.735	0.048	0.217
			A	0.805	0.084	0.111	0.732	0.166	0.102	0.864	0.017	0.119
			B	0.550	0.201	0.250	0.456	0.317	0.227	0.607	0.143	0.250
10	perylene	$C_{20}H_{12}$	P				0.748	0.127	0.125	0.732	0.018	0.251
			O				0.690	0.195	0.115	0.711	0.061	0.228
			A				0.742	0.170	0.088	0.829	0.035	0.136
			B				0.307	0.661	0.032	0.175	0.697	0.127
11	benzo[*m*]tetraphene	$C_{22}H_{14}$	P				0.728	0.147	0.147	0.776	0.028	0.201
			O				0.656	0.185	0.159	0.733	0.049	0.218
			A				0.808	0.135	0.057	0.922	0.007	0.071
			B				0.415	0.316	0.269	0.466	0.216	0.317
			C				0.752	0.210	0.038	0.882	0.042	0.076
12	Kekulene	$C_{48}H_{24}$	P				0.598	0.159	0.243	0.738	0.088	0.174
			O				0.631	0.204	0.165	0.674	0.092	0.234
			A				0.807	0.158	0.035	0.908	0.031	0.061
			B				0.444	0.321	0.235	0.462	0.248	0.289
			in				0.708	0.175	0.117	0.622	0.088	0.290
			out				0.598	0.159	0.243	0.738	0.088	0.174
13	pyrene	$C_{16}H_{10}$	P	0.750	0.096	0.154	0.733	0.109	0.157	0.809	0.010	0.181
			O	0.725	0.147	0.128	0.714	0.157	0.129	0.795	0.042	0.163
			A	0.819	0.154	0.027	0.809	0.168	0.023	0.912	0.028	0.060
			B	0.601	0.210	0.189	0.595	0.213	0.192	0.662	0.131	0.208
14	anthanthrene	$C_{22}H_{12}$	P				0.714	0.106	0.180	0.786	0.012	0.202
			O				0.689	0.169	0.142	0.758	0.061	0.181
			A				0.767	0.185	0.048	0.869	0.040	0.091
			B				0.741	0.205	0.054	0.793	0.119	0.088
			C				0.520	0.230	0.250	0.569	0.167	0.264
15	coronene	$C_{24}H_{12}$	P				0.708	0.124	0.168	0.805	0.018	0.177

DOI: 10.1021/acs.joc.6b01761
J. Org. Chem. 2016, 81, 9669−9686

Table 1. continued

				anharmonic			harmonic					
no.	molecule	formula	R	AI	WS	ALT	AI	WS	ALT	HOMA	EN	GEO
	([6]-circulene)		O				0.731	0.164	0.105	0.808	0.064	0.128
			A				0.735	0.176	0.089	0.816	0.075	0.109
			B				0.780	0.220	0.000	0.768	0.232	0.000
16	ovalene	$C_{32}H_{14}$	P				0.697	0.119	0.184	0.782	0.020	0.198
			O				0.725	0.167	0.108	0.783	0.083	0.134
			A				0.783	0.175	0.042	0.869	0.062	0.069
			B				0.816	0.179	0.005	0.785	0.204	0.010
			C				0.638	0.201	0.161	0.703	0.119	0.178
			D				0.802	0.175	0.023	0.859	0.096	0.045
			10π				0.869	0.131	0.000	0.818	0.176	0.006
17	cyclobutadiene	C_4H_4	P	−1.898	0.295	2.603	−2.104	0.279	2.825	−4.277	0.972	4.305
18	benzocyclobutadiene	C_8H_6	P	−0.098	0.256	0.843	−0.124	0.265	0.859	−0.473	0.160	1.313
			O	−0.028	0.276	0.752	−0.050	0.284	0.766	−0.330	0.163	1.167
			A	0.600	0.110	0.290	0.603	0.102	0.295	0.672	0.000	0.328
			B	−0.827	0.730	1.097	−0.879	0.789	1.090	−1.547	0.980	1.567
19	biphenylene	$C_{12}H_8$	P	0.412	0.270	0.318	0.392	0.269	0.339	0.284	0.073	0.643
			O	0.439	0.287	0.274	0.424	0.285	0.291	0.361	0.085	0.554
			A	0.755	0.133	0.112	0.761	0.125	0.114	0.858	0.000	0.141
			B	−0.429	1.211	0.218	−0.491	1.246	0.245	−0.899	1.349	0.550
20	bicyclo[6.2.0]decapentaene	$C_{10}H_8$	P	0.425	0.216	0.359	0.435	0.200	0.365	0.666	0.002	0.332
			O	0.175	0.346	0.479	0.171	0.332	0.497	0.097	0.076	0.826
			A	0.192	0.217	0.591	0.177	0.208	0.615	−0.165	0.059	1.106
			B	−0.484	1.300	0.184	−0.500	1.290	0.210	−0.798	0.834	0.964
21	tetrakis(cyclobutadieno)-cyclooctatetraene	$C_{16}H_8$	P	−0.247	0.135	1.112	−0.241	0.139	1.102	−0.334	0.087	1.247
			O	−0.466	0.360	1.106	−0.468	0.368	1.100	−0.717	0.356	1.361
			A	−0.633	0.081	1.552	−0.621	0.093	1.528	−1.164	0.146	2.018
			B	−0.602	0.979	0.623	−0.619	0.982	0.637	−0.877	1.012	0.865
22	fulvene	C_6H_6	P	−0.099	0.269	0.831	−0.074	0.080	0.994	−0.199	0.061	1.138
23	pentalene	C_8H_6	P	−0.126	0.230	0.896	−0.158	0.224	0.934	−0.416	0.146	1.270
			O	−0.162	0.314	0.848	−0.190	0.307	0.883	−0.379	0.207	1.172
			A	−0.190	0.390	0.800	−0.215	0.383	0.832	−0.350	0.264	1.086
24	acenaphthylene	$C_{12}H_8$	P	0.516	0.217	0.266	0.504	0.222	0.274	0.564	0.062	0.374
			O	0.591	0.189	0.220	0.582	0.192	0.226	0.643	0.057	0.300
			A	0.792	0.114	0.094	0.789	0.115	0.096	0.883	0.013	0.104
			B	0.272	0.360	0.368	0.254	0.368	0.378	0.242	0.266	0.492
25	pyracyclene	$C_{14}H_8$	P	0.000	0.502	0.498	−0.015	0.497	0.518	−0.049	0.285	0.764
			O	0.226	0.258	0.516	0.220	0.254	0.526	0.222	0.133	0.645
			A	0.589	0.040	0.371	0.606	0.037	0.357	0.761	0.000	0.239
			B	0.060	0.406	0.534	0.040	0.405	0.555	−0.100	0.344	0.756
26	corannulene	$C_{20}H_{10}$	P				0.254	0.576	0.170	0.525	0.249	0.226
	([5]-circulene)		O				0.512	0.281	0.207	0.684	0.098	0.218
			A				0.593	0.185	0.222	0.727	0.049	0.224
			B				0.805	0.195	0.000	0.902	0.098	0.000
27	azulene	$C_{10}H_8$	P	0.662	0.319	0.019	0.674	0.309	0.017	0.991	0.000	0.008
			O	0.516	0.410	0.074	0.522	0.401	0.077	0.722	0.030	0.248
			A	0.533	0.356	0.111	0.530	0.354	0.116	0.571	0.041	0.387
			B	0.199	0.727	0.074	0.205	0.713	0.082	0.395	0.193	0.413
28	heptafulvene	C_8H_8	P	0.229	0.098	0.673	0.274	0.040	0.686	0.204	0.016	0.780
29	pleiadiene	$C_{14}H_{10}$	P	0.580	0.074	0.346	0.582	0.072	0.345	0.600	0.008	0.393
			O	0.480	0.163	0.357	0.480	0.162	0.358	0.540	0.053	0.407
			A	0.582	0.244	0.174	0.584	0.238	0.178	0.705	0.071	0.224
			B	0.119	0.244	0.637	0.112	0.252	0.636	0.146	0.186	0.668
30	[7]-circulene	$C_{28}H_{14}$	P				0.623	0.046	0.331	0.693	0.000	0.307
			O				0.228	0.340	0.432	0.503	0.113	0.384
			A				0.170	0.429	0.400	0.516	0.148	0.336
			B				0.242	0.391	0.367	0.548	0.136	0.316
			C				0.292	0.374	0.334	0.493	0.157	0.350
			D				0.301	0.362	0.337	0.559	0.133	0.309
			E				−0.951	1.933	0.019	−0.196	1.193	0.003

DOI: 10.1021/acs.joc.6b01761
J. Org. Chem. 2016, 81, 9669−9686

Table 1. continued

[a]AI values have been calculated with γ = 6.503 (harmonic vibrational modes) or 7.866 anharmonicity corrected vibrational modes), whereas the HOMA values are determined with α = 282.941. For AI, the bond weakening−strengthening WS and the alternation ALT contributions are given. Also, the analog parameters, the elongation (EN) and the geometry alternation (GEO) of HOMA, are given. The letter P in column ring R denotes the peripheral AI or HOMA value, the letter O denotes the overall values, whereas letters A, B, C, etc. indicate the local values of a ring. All values are calculated at the B3LYP/cc-pVTZ level of theory.

model chemistry used for the calculation of the bond lengths R_i of a given π-systems. Apart from this, the HOMA index is only useful when the Badger rule is strictly fulfilled, i.e., the shorter bond is always the stronger bond, and the local stretching force constant as the only reliable bond strength descriptor is a unique function of the bond length R_i. However, none of these requirements is strictly fulfilled,[82,83] as we will show in this work. The bond length sensitively depends on the charge of the atoms being bonded, and therefore it can happen that the shorter bond is the weaker rather than stronger bond, as has been demonstrated for a large number of bonds between electronegative atoms.[82,83,131] Accordingly, there is no quantitative relationship between bond lengths and intrinsic bond strength, so the use of HOMA as a π-delocalization parameter has to be questioned.

Kalescky and co-workers[117] have suggested in a recent publication to abandon the use of bond lengths and to use instead the more reliable local stretching force constants k_i^a or their associated relative BSO values n_i as direct measures for the intrinsic bond strength. Based on the BSO, a more reliable vibrationally-based aromaticity index (AI(vib); henceforth called just AI) can be defined

$$\mathrm{AI} = 1 - \frac{\gamma}{\mathrm{NB}} \sum (n_{\mathrm{opt}} - n_i)^2 \tag{4}$$

$$\mathrm{AI} = 1 - \gamma\left[(n_{\mathrm{opt}} - n_{\mathrm{av}})^2 + \frac{1}{NB} \sum (n_{\mathrm{av}} - n_i)^2\right] \tag{5}$$

$$\mathrm{AI} = 1 - \mathrm{WS} - \mathrm{ALT} \tag{6}$$

Here, n_{opt} (unitless) is the optimal BSO of Kekulé benzene, n_{av} is the averaged BSO of the target molecule, WS is the weakening−strengthening index of all bonds compared to the average BSO, and ALT is the degree of bond strength alternation. The constant γ (unitless) is equal to 6.503 for BSO values based on harmonic vibrations (n_{opt} = 1.547) and 7.866 when anharmonicity corrections are included (n_{opt} = 1.482). Kaleski and co-workers[117] set up the definition of HOMA and AI in such a way that they both give a value of 1.000 for benzene. However, this is rarely done in the literature, and for reasons of comparison, we follow the common approach of fixing HOMA and AI of Kekulé benzene to be equal to zero. Employing this approach, HOMA and AI of benzene are somewhat smaller than 1.000 (0.998 and 0.924, Table 1).

The AI values determined by the local stretching force constants or their associated BSOs provide the possibility of distinguishing between local and global π-delocalization effects. It is straightforward to calculate the AI value for a specific ring (local π-delocalization), the peripheral π-system, and the global π-system, which includes all bonds. Therefore, local, peripheral, and global AI values are presented for all polycyclic π-systems investigated. In line with other work based on the HOMA approach,[60,61,75,130] we define ranges of AI values as being typical of aromaticity ($0.5 \leq \mathrm{AI} \leq 1.0$), nonaromatic character ($-0.1 < \mathrm{AI} < 0.5$), or antiaromaticity (lower than −0.1). Delocalization indices close to 0 are difficult to interpret, and therefore we lowered the upper bound for antiaromaticity to −0.1.

In some cases, we have extended the investigation from benzeneoide to other rings, which is commonly done in HOMA-based investigations.[130] We will clarify in this work whether such an approach is justified at all.

Geometry optimizations and vibrational frequency calculations were carried out with the B3LYP functional[132,133] utilizing Dunning's cc-pVTZ basis set.[134] Originally, two other functionals were tested (ωB97X-D[135,136] and M062X[137]), but they were excluded because of spurious imaginary frequencies when anharmonicity calculations were carried out (see below). For all DFT calculations, an ultrafine integration grid[138,139] and tight convergence criteria (10^{-8} for the SCF calculations and 10^{-8} atomic units the geometry optimizations) were used to guarantee the accuracy of vibrational frequencies and force constants. For 21 of the 30 conjugated molecules investigated, anharmonically corrected vibrational frequencies have been obtained by using the vibrational perturbational approach.[140,141] Using procedures described elsewhere,[122,142] the anharmonicity corrections were used to obtain anharmonically corrected local stretching frequencies and force constants.

In some cases, the first excited singlet state S_1 was investigated employing time-dependent DFT (TD-DFT).[143,144] TD-B3LYP/cc-pVTZ geometries and vibrational frequencies were used to derive TD-B3LYP local mode properties and the corresponding AI values. All local mode and AI calculations were carried out with the program package COLOGNE2016.[145] For the DFT calculations, Gaussian 09, rev C1,[146] was used.

3. RESULTS AND DISCUSSION

In Table 1, the AI values calculated in this work for conjugated π-systems **1**−**30** (Figure 2; there also a numbering of C atoms as used in this work is given) are compared with the corresponding HOMA indices based on optimized CC bond lengths. Where possible, the harmonic description was replaced by the anharmonically corrected one. For each molecule, the bond strengthening/weakening term and the bond alternation term (WS and ALT in the case of local stretching force constants k^a; EN and GEO in the case of calculated CC bond lengths) are given. The validity of the extended Badger rule is tested in Figure 3 for CC and CH bonds. Figure 4 gives the relationship between relative bond strength orders (BSOs) for CC and CH bonds. Kekule benzene was modeled by using the CC bonds of *trans*-1,3-butadiene (see Supporting Information).

In the following discussion, we will address (poly)cyclic, fully conjugated hydrocarbons as being aromatic if the AI value fulfills the condition $0.5 \leq \mathrm{AI} \leq \mathrm{AI(benzene)}$, nonaromatic for $-0.1 \leq \mathrm{AI} < 0.5$, and antiaromatic for all $\mathrm{AI} < -0.1$. This implies that AI values > AI(benzene) would indicate superaromaticity. In special cases, we will complement the AI analysis by giving the BSO values of individual CC bonds, which are all summarized in the Supporting Information.

Choice of the Reference. Roth and co-workers[147,148] have shown that the choice of the reference can be essential when discussing the delocalization energy of a cyclic π-conjugated molecule. Using the heats-of-formation of *trans*-1,3-butadiene[119] and the homodesmotic eq 7:

$$\text{benzene} + 3 \times \text{ethene} \rightarrow 3 \times \textit{trans}\text{-1, 3-butadiene} \tag{7}$$

leads to an aromatization energy of 19.8 kcal/mol for benzene, whereas *cis*-1,3-butadiene gives a value of 25.4 kcal/mol. Clearly, *cis*-1,3-butadiene is better suited when comparing with a cyclic π-system. However, the cis-form does not correspond to a stable form, as it is the transition state (TS) for the rotation of 1,3-butadiene from one gauche local minimum into the other. Exchange repulsion involving the endocyclic CH bonds of the terminal groups increases the cis-energy, which has to be considered when using this form as a reference.[147,148] In the case of the local mode approach, the use of the cis-form as a

DOI: 10.1021/acs.joc.6b01761
J. Org. Chem. 2016, 81, 9669−9686

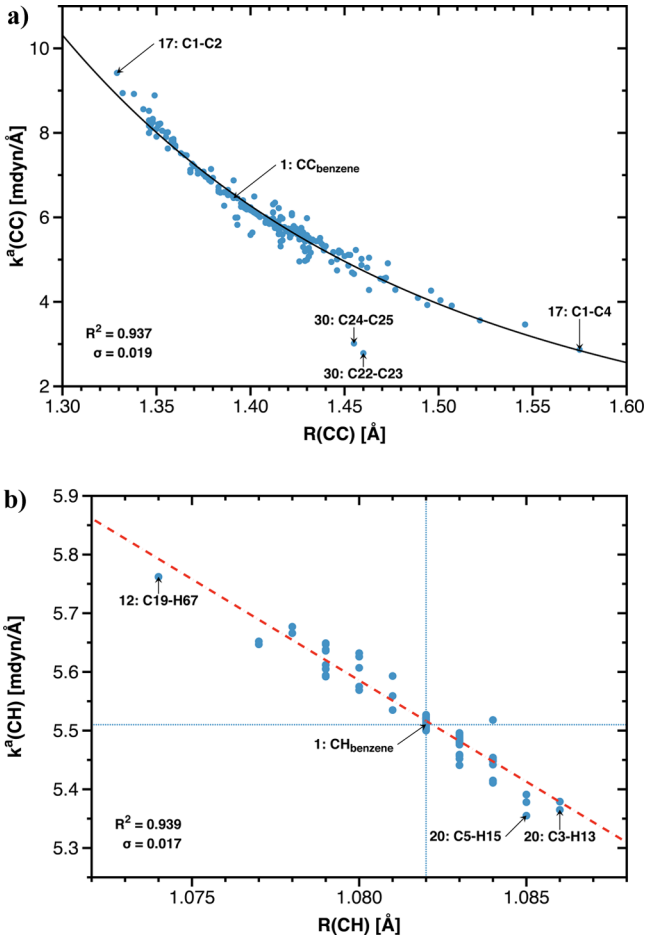

Figure 3. Testing the extended Badger rule: (a) Correlation of the CC local stretching force constant k^a [mdyn/Å] with the CC interatomic distances R [Å] (R^2 = 0.937, σ = 0.019) and (b) the CH local stretching force constants with the CH bond lengths (R^2 = 0.939, σ = 0.017). B3LYP/cc-pVTZ calculations.

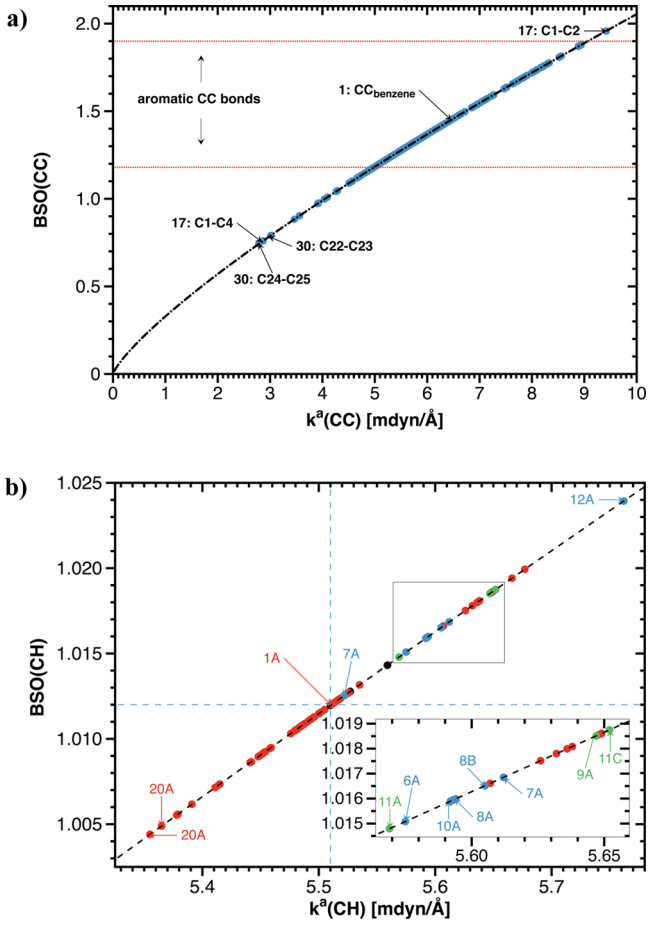

Figure 4. Correlation of the (a) relative CC BSO with the CC local stretching force constant k^a(CC) [mdyn/Å] and (b) of n(BSO) with k^a(CH) . The red, blue, and green dots correspond to the peri-, bay-, and U-positioned hydrogens, respectively. Numbers of the molecule and the ring are also given (as provided in Figure 2). B3LYP/cc-pVTZ calculations.

reference implies that the corresponding imaginary frequency and its associated normal mode is projected out. We have used both the trans- and the cis-form of 1,3-butadiene as reference to model Kekulé benzene. As can be seen from the data in Table 2, results are almost identical for the two different references, which makes us conclude that the calculation of the AI based on the local stretching force constants is a robust method that correctly provides trends of AI values irrespective of the reference chosen.

AI versus HOMA. The AI and HOMA indices would be identical if the Badger rule would be exactly fulfilled. However, this is not the case, as is shown in Figure 3. There is a power relationship between local CC stretching force constant and CC bond length for the range of values between the CC single and the CC double bond in **17** (cyclobutadiene), as anticipated by Badger.[128] However, the correlation constants (R^2 = 0.937; σ = 0.019) reveal that there is a relatively strong scattering of data points so that this correlation is just qualitative for the CC bonds. In recent work, it has been shown that in the case of bond anomalies, the Badger rule is violated in the sense that the shorter bond turns out to be the weaker bond and vice versa.[82,83] Especially for strained ring molecules or polycyclic systems, which involve a charge transfer from one ring to the other to obtain aromatic electron ensembles (see **30** in Figure 3), CC bond lengths provide an inaccurate measure of the CC bond strength and the degree of π-electron delocalization. Accordingly, the correlation of the HOMA values with the more reliable AI values is just moderate, leading to R^2 values of 0.747 to 0.743 and relatively large standard deviations σ caused by some outliers in connection with nonbenzoide cyclopolenes (Tables 1 and 2).

The deviations between HOMA and AI are preferentially due to a different description of antiaromatic systems for which the HOMA index largely exaggerates the antiaromatic character. We will later show that this is due to an exaggeration of the bond alternation term.

Table 2. Comparison of Different Aromaticity Descriptors

	AI^{trans}	AI^{cis}	HOMA^{trans}	HOMA^{cis}
AI^{trans}		0.997	0.743	0.722
AI^{cis}	0.032		0.763	0.747
HOMA^{trans}	0.431	0.414		0.995
HOMA^{cis}	0.335	0.319	0.042	

[a]The table contains results in form of a matrix. The upper right triangle of this matrix gives the correlation coefficients R^2, whereas the lower triangle contains the standard deviation σ. AI and HOMA descriptors are determined utilizing a Kekulé either based on *trans*- or *cis*-1,3-butadiene. B3LYP/aug-cc-pVTZ calculations.

DOI: 10.1021/acs.joc.6b01761
J. Org. Chem. 2016, 81, 9669−9686

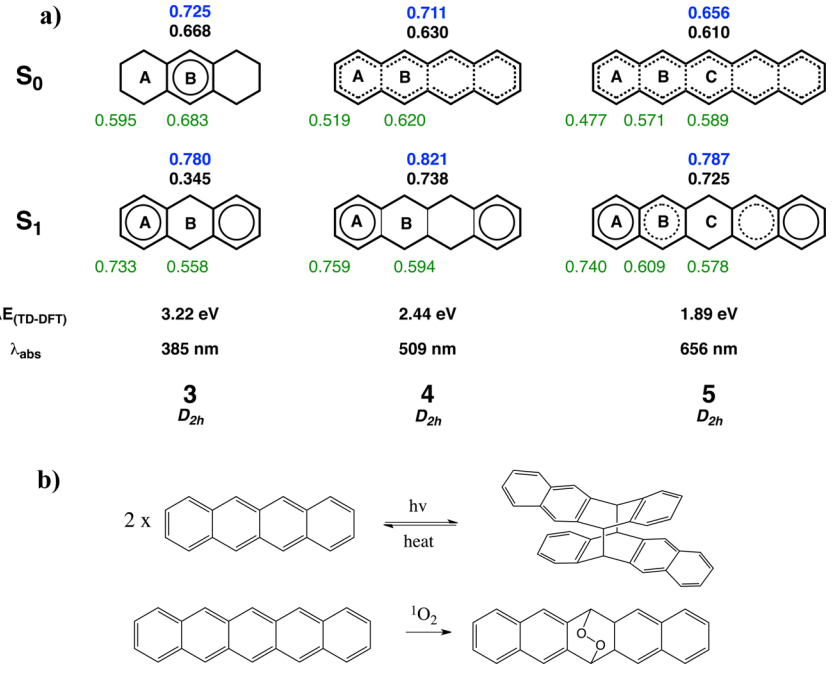

Figure 5. (a) Comparison of the AI values for the S_0 ground state and the S_1 excited state of acenes **3**−**5**. Geometry and vibrational frequencies of the S_1 states were calculated at the TD-B3LYP/cc-pVTZ level of theory. Green numbers give the AI for an individual ring (A, B, etc.), blue numbers give the peripheral AI value, and black numbers give the global AI. (b) Reactions of [4]acene and [5]acene.

In the case of the CH bonds, the Badger rule is also poorly fulfilled (R^2 = 0.939, σ = 0.017 Å). Despite of a small variation in the bond length from 1.074 to 1.086 Å, strain effects (e.g., in the case of peri H atoms or bay CH-bonds) cause a variation of the local CH stretching force constant from 5.35 to 5.75 mdyn/Å (Figure 3, lower half).

Use of Experimental Frequencies. In previous work, it was found that experimental frequencies lead to similar BSO values as those obtained from vibrational frequencies based on the harmonic approximation.[84,85] This resulted from the fact that for both reference and target molecules, the anharmonicity corrections had about the same magnitude if one particular bond type was considered. In the current work, this is no longer the case, as the anharmonicity correction for the CC double bond in 1,3-butadiene is different from that in benzene or that of a single bond in ethane. As long as just aromatic benzoide hydrocarbons are compared, the anharmonicity corrections lead to relatively small changes in the AI value. Small as well as larger changes for the antiaromatic molecules (**17**: +0.206) are possible (Table 1), where most changes lead to the effect that aromatic molecules become somewhat less aromatic and antiaromatic molecules become significantly more stabilized. In the latter case, the bond alternation term turns out to be exaggerated by the harmonic approximation. In other cases, only a careful analysis of the WS and ALT terms reveal which of these is decisive for weakening the (anti)aromatic character of a molecule.

In the following, we will use the harmonic AI values because these are available for all molecules investigated. However, we will discuss only trends in calculated AI values and refrain from discussing absolute AI values because these can be subject to a larger anharmonicity correction (change in the k^a values of butadiene from 9.089 and 5.040 to 8.663 and 4.655 mdyn/Å due to anharmonicity; the BSO values decrease from 1.909 and 1.191 to 1.874 and 1.090, respectively) as seen for conjugated π-systems such as **4**, **7**, or **17**.

π-Delocalization in Acenes. Acenes are benzoide hydrocarbons with linearly fused benzene rings.[149,150] Naphthalene (**2**: [2]acene), anthracene (**3**: [3]acene), tetracene (**4**: [4]acene), and pentacene (**5**: [5]acene) have been investigated in this work (see Figure 2 and Table 1). It is known that acenes are thermodynamically less stable than their ortho-fused counterparts of which phenanthrene (**6**: [3]helicene) is the first[117] and benzo[c]phenanthrene (**9**: [4]helicene) is the second member. The difference in thermodynamic and kinetic stability between these two groups of benzoide hydrocarbons can be traced down to their aromatic character (thermodynamic stability) and to the nature of their frontier orbitals (reactivity). The acenes **2**−**5** correspond to 10, 14, 18, and 22 π-systems, which according to the calculated AI prefer to delocalize peripherally (blue AI values in Figure 5), where the magnitude of AI decreases exponentially (**2**: 0.775 ; **3**: 0.725; **4**: 0.711; **5**: 0.656), asymptotically approaching a value of 0.60, which implies that the acene reactivity increases to a limit with the number of benzene rings as the aromaticity decreases to a minimum which, according to our calculations, has still (weak) aromatic character.

Starting with anthracene, the inner ring (ring B) has a larger AI than the outer rings (ring A): 0595 (outer) vs 0.683 (inner); [4]acene: 0.519 vs 0.620; [5]acene, outer: 0.477; inner: 0.571, 0.589. This is in line with the picture of inner 6π (**3**; **5**) or 10π units (**4**), which are extended to the outside by 4π-diene units. The decrease in the aromaticity of the inner benzene (naphthalene) units is parallel to that in the peripheral $(4n + 2)\pi$-delocalization (n = 2, ..., 5).

It is well-known that the reactivity of acenes increases with the number of linearly annulated benzene rings. (4 + 4) or (4 + 2) Cycloadditions are typical reactions of the acenes, where the innermost aromatic benzene ring is the center of reactivity contrary to its increased aromatic character. This can be explained as being kinetically, rather than thermodynamically, controlled. The largest coefficient of the HOMO and the

DOI: 10.1021/acs.joc.6b01761
J. Org. Chem. 2016, 81, 9669−9686

LUMO can be found for carbons 5 and 10 of anthracene (see Figure 2), which suggests that charge polarization or charge transfer affects these C atoms irrespective of the fact that the central ring in anthracene has the highest AI. The frontier orbitals of **4** and **5** lead to similar conclusions.

The higher acenes ([4]-acene and [5]-acene) dimerize under the influence of visible light, which indicates that excitation to a low-lying singlet state is facilitated with increasing *n*. Figure 5 gives the results of TD-B3LYP calculations for the S_1 state of **3**, **4**, and **5** (intersystem crossing is excluded here). The excitation energies decrease from 3.22 to 2.44 and 1.89 eV in line with the fact that the higher acenes are already sensitive to visible light.[150] For anthracene, a drastic reduction of global delocalization from 0.668 (S_0) to 0.345 (S_1) is calculated, which is due to the occupation of a LUMO with 5,12 (5,13) antibonding character, thus interrupting peripheral delocalization. Rings A (outer rings) have strongly increased AIs of 0.733 (compared to 0.595), whereas ring B has a reduced AI of 0.558 (compared to 0.683 in the S_0 ground state). This suggests an electronic structure related to a 9,10-biradicaloid that easily undergoes cycloadditions, for example, with singlet oxygen to form 9,10-endoperoxide and other 9,10-derivatives.[151]

In general, the delocalization patterns of the S_1-excited states of the acenes are reversed (Figure 5): The outer rings have now the higher AI values, whereas the inner rings B and C are just weakly aromatic: [4]acene: 0.759 vs 0.594; [5]acene: 0.740 vs 0.609 vs 0.578. This confirms the description of the S_1-state of the [n]acenes as biradicaloids reacting preferably with their central C atoms, as shown for two examples in the lower part of Figure 5. Cycloadditions lead in the case of the [4]acene to a stable benzene and naphthalene unit and in the case of [5]acene to two stable naphthalene units, which explain the high reactivity under photochemical conditions.

Noteworthy is that in the S_1 state, there is an increased peripheral delocalization higher than that in the ground state: 0.780, 0.821, 0.787 (S_0: 0.725, 0.711, 0.656). This implies that excited states can be more aromatic than the ground state. The all-bond analysis reveals that [3]acene **3** has compared to [4]acene **4** a strongly reduced local π-delocalization in ring B (AI = 0.558 compared to 0.683 in the S_0 state; Figure 5 and Table 1)

Benzoide Molecules Related to Phenanthrene. Phenanthrene can be viewed as the first member of the [*n*]-helicenes or the starting point of the zig-zagging phenacenes, such as **8**. Apart from this branching topologies (**7**), cyclic topologies other than helicenes (e.g., **11**) and their complementation to Kekuléne (**12**) or doubling of the phenanthrene core as in perylene (**10**) are possible. Common to all these topologies is that (1) benzene units with high AI values can be formed that have higher AI values than result from peripheral π-delocalization and (2) bay CH bonds exist that because of space confinement are compressed and therefore are stronger than normal CH bonds.

It is well-known that phenanthrene is 6.8 kcal/mol more stable than anthracene according to measured heats of formation $\Delta H_0^f(298)$ of 48.2 and 55.0 kcal/mol.[152,153] In recent work by Kalescky and co-workers,[117] it was demonstrated that the larger stability is due to the fact that **6** can establish two aromatic benzene units, whereas **3** can form only one (ring B), which is in line with Clar's rule.[36] The C12C13 bond in **6** has a BSO value of 1.204, which is somewhat larger than that of the central bond in (1.191 for trans and 1.142 for cis). The strong alternation suggests that ring B of **6** is nonaromatic (AI = 0.477 < 0.500) characterized by the strong C9C10 double bond (BSO: 1.728).

In the chrysene ([4]phenancene, **8**), the terminal A rings have decreased aromatic character (AI: 0.777 vs 0.795 in **6**). Its peripheral conjugation is also less developed than in [3]-phenancene (0.670 vs 0.718) which results from the fact that an 18π-system has smaller tendency to delocalize than a 14π-system. This is also reflected by the higher AI for ring B (0.550 vs 0.477). Although chrysene has only two benzene units compared to the three of triphenylene, the heat-of-formation describes the former (63.0 kcal/mol, Figure 5) somewhat more stable than the latter (65.5 kcal/mol), which is a result of the larger π-delocalization in ring B (AI = 0.550 compared to 0.354 in **7**). Another factor should be the presence of three bay CH pairs in **7** compared to just two in **8**. The resonance energy of **7** has been estimated to be 80.7 kcal/mol,[147] whereas that of of **8** should be 83.2 kcal/mol due to the establishment of a less-branched 18π-system.

Benzo[*c*]phenanthrene (**9**) has because its U-shaped form strong exchange interactions between the two bay-oriented CH bonds. It is the least stable of the three 18π-systems **7**, **8**, and **9**, ($\Delta H_0^f(298)$ = 69.6 compared to 63.0 and 65.5 kcal/mol in the case of **8** and **7**, respectively).[119,154] Its peripheral delocalization (0.628) is the lowest obtained. Ring A has an AI of 0.732 (**8**: 0.777), and the AI of ring B is down from 0.550 to 0.456 (BSO values of ring B: 1.087 for the bay bond C16C17, 1.236, 1.339, 1.763, 1.309, 1.309 (clockwise around the ring).

Perylene (**10**, $C_{20}H_{12}$) is best viewed as two naphthalene units (each A-ring: 0.742; **2**: 0.726) loosely connected via bonds C13C14 and C16C17 (BSO: 1.166) to a 20π-system should have in its periphery 18π-electrons, which is confirmed by a relatively high peripheral AI of 0.748 and a much lower all-bond AI value of 0.690.

Benzo[*m*]tetraphene (**11**) has similar to **9** U-shape, however because of the insertion of ring C between the two B rings, the U is broader without the close CH contacts at the end of the U-legs. Rings A and C have relatively high local aromaticity (AI: 0.808 and 0.752), whereas ring B is nonaromatic (0.415 vs 0.456 in **9**). Molecules **6**−**11** indicate that local aromaticity is stronger than peripheral or global delocalization when one string of benzene units exist. However, when two (partial) strings exist as in **10**, Clar's rule is no longer valid, as more stable naphthalene units or peripheral delocalization develop.

The most stable structure of Kekuléne, (**12**) $C_{48}H_{24}$, turns out to have D_{3d} symmetry as in an annulene with inner 18π and outer 30π delocalization cycles, rather than D_{6h} symmetry (arrangement of 6 overlapping phenanthrene units leading to 6 benzene units equal to ring A in **4**) as was suggested by Jiao and Schleyer.[155] The symmetry lowering is a result of the fact that the inner 6 CH bonds alternate to point out of the ring plane. The calculated AI values for the six A rings are 0.807, which is somewhat larger than the corresponding phenanthrene value (0.795), whereas in ring B (0.444), π-delocalization is somewhat less than in phenanthrene (0.477), thus confirming that the 6 benzene units are more developed than in **6**. If one compares the inner 18π with the outer 30π delocalization (both comply with Hueckel's (4*n* + 2) rule), then the former is stronger delocalized (AI = 0.708) than the latter (AI = 0.598), which is in line with an exponential decrease of aromatic stabilization with increasing *n*. The average AI per bond is 0.662 for the phenanthrene-built structure and 0.583 for the annulene structure, thus confirming that the D_{3d}-symmetrical form of Kekuléne is the thermodynamically more stable one. The

DOI: 10.1021/acs.joc.6b01761
J. Org. Chem. 2016, 81, 9669−9686

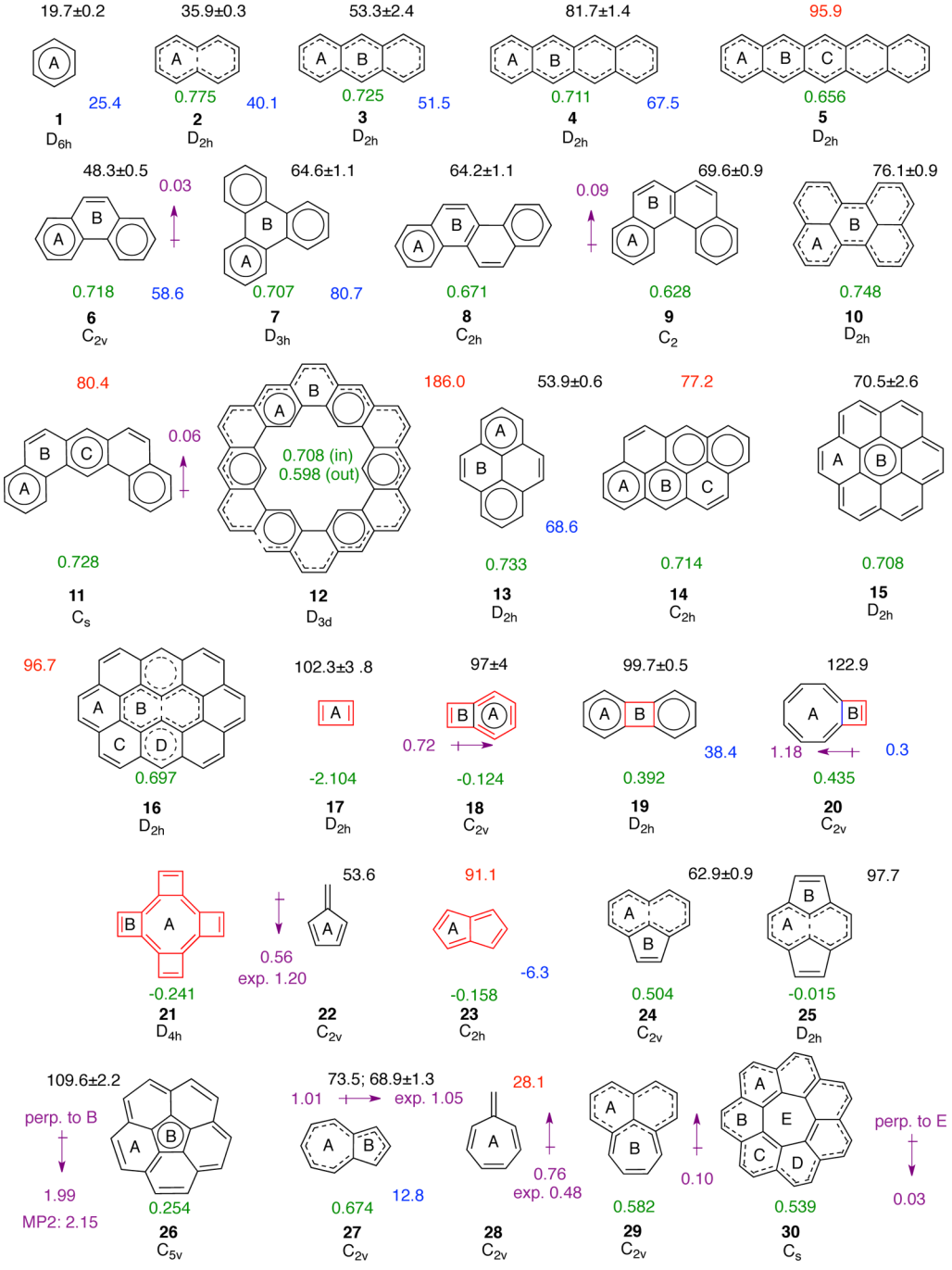

Figure 6. Preferred delocalization modes either following Clar's rule or forming larger units when naphthalene units or peripheral delocalization is preferred. Peripheral AI values are given in green below each molecule. Antiaromatic molecules or units are given in red. Black numbers are heats-of-formation, red numbers are calculated or estimated values, and blue numbers are resonance energies (all energy values in kcal/mol). For a complete list of references, see SI. Dipole moments (in Debye) are indicated by a purple arrow oriented in the direction of the largest negative charge. Exp., experimental; perp., perpendicular.

HOMA fails as it predicts stronger aromaticity for the outer than the inner cycle (0.738 vs 0.622), which is a result of exaggerating bond alternation for the inner cycle.

The calculated AI values do not provide any support for superaromaticity of Kekuléne, which was preciously suggested in view of high extra stabilization energies obtained with HF calculations and small basis sets. Superaromaticity would imply extra-stabilization (exceeding that of suitable reference molecules)[155] along with an AI value larger than that of benzene (AI = 0.926). This is not the case; therefore, the vibrational properties of **12** suggest 6 overlapping phenanthrene structures yielding 6 local benzene units. Or in other words: Local aromaticity leads to a larger stability than a global π-delocalization involving 18 (inside) and 30π-electrons (outside). Hence, the probing of the CC bonds via their local stretching modes by an infinitesimally small change of the bond turns out to be sensitive and precise.

It is interesting to compare the delocalization of the inner cycle of Kekuléne with that of a D_{6h}-symmetrical [18]annulene (R values of 1389 and 1.406; BSO values of 1250 and 1.406).

DOI: 10.1021/acs.joc.6b01761
J. Org. Chem. 2016, 81, 9669−9686

The HOMA value is 0.991, suggesting a large aromaticity that is not confirmed by any other investigation of [18]-annulenes.[156−159] Schleyer and co-workers[158] found that corresponding to the DFT method used, a C_2-symmetrical form with considerable bond alternation was the most stable. Ivanov and Boldyrev[160] calculated, in agreement with our result, the D_{6h}-symmetrical form to be more stable. They described π-delocalization in the form of a strong alternation of three two-electron- and six three-center-two-electron-delocalization units that are in line with its polyene-like character.[161] This is also in line with the AI value of 0.133 calculated in this work.

CH bonds of benzenoide molecules have a BSO value of 1.12 ± 0.01. BSO(CH) values are remarkably constant unless steric effects (in the sense of four-electron destabilization described by perturbational MO theory) lead to a change in the intrinsic bond strength. Peri-CH bonds, as in naphthalene, are reduced in their BSO to 1.09 or 1.10. Space confinement, as it occurs in bay regions, leads to increased BSO values: phenanthrene (**6**), 1.015; perylene (**10**), 1.016; [2H$_{12}$]chrysene (**8**), 1.016 and 1.017; benzo[*c*]phenanthrene (**9**), 1.019 (H atoms are out of the carbon plane); benzo[m]tetraphene (**11**), 1.015 and 1.019; Kekuléne (**12**), 1.024 (inner H atoms; they are above and below the carbon plane). This reveals that the CH BSO values (based on the local CH stretching force constants) sensitively reveal space confinement effects, which can vary between 1.015 and 1.024.

Benzoide Molecules Related to Pyrene. Pyrene (**13**) can be considered as a phenanthrene for which the bay region is bridged by a C_2 unit. The peripheral delocalization index is 0.733, which is compared to that of ring A (0.809) significantly lower, thus indicating local aromaticity rather than the establishment of a 16π antiaromatic π-system. Bonds C4C5 and C9C10 have a similar double-bond character (BSO: 1.721) as the corresponding bond in **6** (1.728) and are only weakly linked (1.268 vs 1.280 in **6**) to ring A.

The topology of anthanthrene (**14**, $C_{22}H_{12}$) is related to that of pyrene as well as chrysene: Two aromatic A rings (AI: 0.767; 0.809 in **13**) are connected by rings B (0.741) and C (0.520), where the latter is related to ring B in **13** as reflected by a C4C5 and C10C11 BSO value of 1.757 (1.721 for **13**). The chrysene topology becomes obvious if one follows the pattern A−B−B−A and considers rings C as closing the bay regions of chrysene. The peripheral delocalization is relatively high (AI = 0.714) because an aromatic 18π-system with an internal 4π-unit can be formed (C19C20C21C22; BSO values: 1.407, 1.423, 1.407).

Coronene (**15**, $C_{24}H_{12}$) is a [6]-circulene with a central 6π benzene unit B (AI = 0.780) and a peripheral 18π-system (AI = 0.708), where each A ring has an AI value of 0.735, i.e., local and global π-delocalization are balanced, which is also reflected by the fact that the HC═CH units have a relatively low double-bond character of 1.628. One can view the molecule also as two superimposed triphenylenes, which enforce π-delocalization for the inner 6- and the outer 18-ring. Ovalene (**16**, $C_{32}H_{14}$) is formally an antiaromatic 32π-system, which however is closely related to coronene insofar as it is a peripheral aromatic 22π-system (AI: 0.697) with an internal 10π naphthalene unit (AI of B: 0.816; B + B 10π-system: 0.869), which is stronger aromatic than naphthalene itself (*P* value of AI: 0.775). The outer rings A, C, and D have relatively high AI values (0.783; 0.638; 0.802) with low HCCH BSO values in A and C: 1.561, 1.695. As in the case of coronene, local and global aromaticities are well-balanced. It is interesting that the HOMA index describes the system as four overlapping phenanthrene units leading to four Clar sextets (see Figure 6), i.e., two rings A and two rings D (0.869, 0.859). The AI leads to a pyrene unit with the central naphthalene unit and the D ring having an AI of 0.802. It seems that the HOMA index because of its lower sensitivity ignores the possibility of an inner 10π-delocalization that can also not be predicted on the basis of Clar's rule. As in the cases of **10** and **15**, Clar's rule does not hold for **16**.

π-Delocalization in Molecules Containing the Cyclobutadiene Unit. The prototype of an antiaromatic molecule is cyclobutadiene (**17**), and not much more can be said about this system that is not already discussed in the literature.[162−176] Its AI is −2.104, which after anharmonicity corrections becomes −1.898 (Table 1). The strongly negative value is due to the large bond alternation term (2.825; anharmonically corrected: 2.603), whereas the bond length change contributes only 10%.

Cyclobutadiene has no alternative delocalization mode. Polycyclic cyclobutadienes such as molecules **18**−**21** can adopt delocalization modes, which avoid the formation of an antiaromatic 4*n* π-delocalization unit. In benzocyclobutadiene (**18**), this is accomplished by forming an aromatic benzene ring (AI: 0.807) complemented by a double bond in a four-membered ring (BSO: 1.808) that is only weakly linked to the benzene unit via single bonds (BSO: 0.903), so that an antiaromatic peripheral 8π-delocalization is largely suppressed (AI: −0.124; −0.098 anharmonically corrected). If only delocalization in the four-membered ring is considered, then the antiaromatic AI value is reduced from −2.104 to just −0.879 (Table 1).

In case of biphenylene (**19**), a total of 12π-electrons has to be delocalized over three rings so that any antiaromatic grouping of electrons is avoided. This is accomplished by establishing two benzene rings (AI: 0.761) and a four-membered ring (BSO values: 0.973 and 1.326) with 4 excocyclic double bonds (BSO: 1.569). In this way, the 4-ring AI values are reduced to −0.491 (absolutely seen), and the peripheral delocalization index of 0.392 describes a nonaromatic π-system.

The situation is different for **20**, as in this case, a peripheral 10π-system can be established.[177] For the eight-membered ring A, an AI of 0.177 is obtained, suggesting a nonaromatic system (BSO values: 0.883 (C9C10), 1.719, 1.220, 1.558, 1.175), whereas for ring B, reduced antiaromatic character is suggested by an AI value of −0.500 (BSO: 0.883 (C9C10), 1.175, 1.336). The all-bond AI and the peripheral AI are 0.171 and 0.435, respectively, which is typical of a nonaromatic system with distinct bond alternation (ALT = 0.497) and bond length changes (WS = 0.332). Ring B has two exocyclic double bonds and can reduce in this way its antiaromatic character.

Tetrakis(cyclobutadieno)cyclooctatetraene (TCCO) **21** is an antiaromatic 16π-system, which, contrary to **20**, cannot rearrange its π-electron system in such a way that it avoids antiaromatic electron ensembles. The reduction of the antiaromatic character of the four-membered rings is the driving force, which forces double bonds into exocyclic positions and establishes in this way an antiaromatic eight-membered ring. The peripheral AI value is −0.241, thus suggesting reduced antiaromaticity compared to the AI values of ring A and rings B (−0.621 and −0.619). Again, this confirms that overall peripheral π-delocalization always reduces the destabilizing π-interactions of the individual rings. Noteworthy is that anharmonicity corrections change the AI values

DOI: 10.1021/acs.joc.6b01761
J. Org. Chem. 2016, 81, 9669−9686

of ring A and ring B to −0.633 and −0.602, respectively, without changing the peripheral delocalization much (−0.247 vs −0.241, Table 1). Obviously, it is more effective for the stability of the molecule to reduce the antiaromaticity of four cyclobutadiene units rather than one cyclooctatetraene unit.

The large deviations between AI and HOMA values are preferentially due to the description of antiaromatic π-systems. HOMA exaggerates the bond alternation terms, which results in an overestimation of the antiaromatic character of a molecule: cyclobutadiene: −4.277 compared to −2.104. Clearly, this is a result of the large value of the constant α in eq 1 (282.9 compared to 6.503), which has to enlarge bond length differences to meet the whole span of HOMA indices from the most extreme (anti)aromatic values, which are more difficult to describe with a first-order property (bond lengths) than a sensitive second-order property.

π-Delocalization in Molecules Containing the Fulvene Unit. The calculated AI value of fulvene (**22**, −0.074) describes the system as being nonaromatic with a small negative value of A due to the fact that just 5 electrons are in the ring. By charge polarization of the exocyclic double bond the ring becomes slightly negative, thus leading to a dipole moment of 1.20 D[178] (BSO values: exo: 1.876; internal: 1.089, 1.762, 1.101). It is well-known that electron-donating substituents can lead to an aromatic five-membered ring.[179] In this work, the focus is on π-systems containing the fulvene unit such as the C_{2h}-symmetrical pentalene (**23**), where charge polarization does no longer exist. A peripheral 8π-system exists, which is weakly antiaromatic (AI = −0.158; ring A: −0.215) where anharmonic corrections lead to a 15% reduction of the antiaromaticity. The HOMA value of −0.315 is exaggerated due to the large bond alternation term (Table 1). In view of the fact that for 1,3,5-tri-*tert*-butylpentalene an antiaromatization energy of −6.3 kcal/mol was determined, the smaller AI value is more reasonable rather than the exaggerated HOMA value.

Acenaphthylene (**24**), pyracylene (**25**), and corannulene (**26**) contain the fulvene unit. In the first case, the naphthalene unit is maintained (AI of ring A: 0.789 vs AI(**2**): 0.748), whereas the 5-ring B has a low AI of 0.254 due to a strongly localized double bond (BSO values: 1.097, 1.684). Noteworthy is that the exocyclic fulvene bond, which becomes now the central bond of the naphthalene unit has a BSO value of 1.524, and thereby it is much stronger than the central bond of naphthalene (BSO: 1.290). This picture emerges also from the AI values of pyracylene (ring A: 0.696; ring B: 0.040; BSO values in ring B: 1.009, 1.669). The central bond has a BSO value of 1.870, thus suggesting an introverted naphthalene unit where the central bond has the highest rather than the lowest π-character in the sense that a central 6π unit of C9C12(C13═C14)C10C11 (2 × [4 × 1.457 + 1.870 − 5] = 5.26 π-electrons; see Supporting Information) dominates the electronic structure of **25**, thus avoiding the antiaromatic peripheral 12π-electron delocalization by establishing a nonaromatic (AI: −0.015).

Corannulene (**26**) has a nonplanar structure (therefore coined *buckybowl*) with a barrier to planarity of 10.2 kcal/mol.[180] One can inscribe a sphere of radius 6.462 Å corresponding to a curvature of 0.154 $Å^{-1}$ for the bowl form of corannulene. Since Kekulé-benzene is a poor reference for the molecule (see below), we point out here just some qualitative features: In the periphery of the molecule, there are formally 15π-electrons. The interior of the molecule is best described as a [5]radialene so that an interior 5π-system couples with an exterior 15 π-system. This leads to a charge transfer from the exterior to the interior cycle, thus establishing two quasi-aromatic cycles and a molecular dipole moment of 1.99 D (downward toward the 5-ring oriented; 2.15 at the MP2/6-31G(d) level of theory).[181] Accordingly, the inner-cycle AI (0.805; formally for 6π-electrons) is unusually high, whereas the outer-cycle AI (0.254; formally for 14π-electrons) is relatively low and nonaromatic. Of course, these values contain strain effects, which might exaggerate the aromatic character. Noteworthy is that the HOMA values again overestimate the degree of aromaticity (0.902 and 0.525, Table 1).

Azulene (**27**) is known as an aromatic isomer of naphthalene, which again results from the fact that the 7-ring donates charge to the 5-ring as reflected by the molecular dipole moment of 1.01 D (exp: 1.05 D)[182] oriented from ring A (positively charged) to B. The HOMA as the less sensitive parameter gives a peripheral delocalization index of 0.991 (7-ring: 0.571, 5-ring: 0.395; Table 1) which is clearly too high. The peripheral AI value is 0.674, that of the 7-ring 0.530 and of the 5-ring 0.205, where the latter value is probably underestimated because of ring strain showing up in a relatively large WS contribution (0.713) as the vibrational properties are sensitive to strain effects. Apart from this, both descriptions suggest peripheral 10π-delocalization with a weak central bond (BSO: 1.042), where the AI value is in agreement with an aromatization energy of 12.8 kcal/mol.[147]

π-Delocalization in Molecules Containing the Heptafulvene Unit. Heptafulvene (**28**) has the opposite double-bond polarization than (penta)fulvene (dipole moment: 0.76 D; exp. value: 0.48 D),[183] i.e., from the ring to the terminal CH_2 group, which is less effective. Accordingly, the peripheral delocalization is weak, which is typical of a nonaromatic molecule (0.274). Pleiadiene (**29**) can be considered as a butadieno-bridged naphthalene, which gets some local aromaticity because of the latter: peripheral AI: 0.582, ring B: 0.112, but each of rings A: 0.584. By this, the local aromaticity is comparable to that of acenaphthylene, but larger than that of azulene.

Circulene ([7]-circulene, **30**) belongs together with corannulene ([5]-circulene), coronene ([6]-circulene), and Kekuléne in the same class of conjugated molecules, which however have different geometries and delocalization properties. [7]-Circulene is nonplanar, has C_2-symmetry, and a saddle-shaped overall structure, i.e., it is nonplanar[184] and the same restrictions with regard to the use of Kekulé-benzene as reference molecule as in the case of corannulene hold. However, even on a more qualitative basis, the 28π-system can be split up into an inner 7π ring, which is electron donating and an outer 21π-ring which is electron accepting thus leading to a tiny dipole moment of 0.03 D. In line with this is that ring E becomes antiaromatic (AI: −0.951), whereas the six-membered rings all adopt nonaromatic character (AI: 0.170−0.301). However, there seems to be a peripheral aromatic delocalization as suggested by an AI of 0.623. This is in line with what is available so far on **30**, for which an inner paratropic coupled to an outer diatropic ring current has been found.[27,185,186]

Advantages, Limitations, and Pitfalls of the AI Based on Vibrational Modes. The advantages of the AI approach presented in this work are (i) the high accuracy provided by the vibrational spectroscopic data, (ii) the general applicability, (iii) its better physical foundation (use of the intrinsic bond strength rather than bond lengths), and (iv) the possibility of starting from measured vibrational frequencies or calculated ones. In

DOI: 10.1021/acs.joc.6b01761
J. Org. Chem. 2016, 81, 9669−9686

the former case, shortcomings of the harmonic approach or the quantum chemical method and basis set used are eliminated, which makes the method particularly attractive.[117] In general, a vibrational frequency can be more accurately determined than a bond length, which is measured as r_z, r_s, r_0, r_g, r_a, etc. value but never as r_e value.

In the case of high frequencies, one can assume that the lowest vibrational eigenstate is predominantly populated so that the frequency is available with high accuracy. The procedures worked out by Cremer and co-workers always guarantee that the normal-mode frequencies are converted in local mode frequencies and force constants without a loss of accuracy.[122] A similar conversion into r_e values is tedious and cannot be generally carried out for larger molecules. Apart from this, it has been shown that bond lengths do not necessarily reflect the intrinsic strength of a bond, as the Badger rule is not fulfilled in many cases.[82,83,131] However, the local mode stretching force constant does as has been shown in a basic derivation of the intrinsic bond strength from local stretching force constants.[127]

Apart from these basic considerations, both HOMA and AI are misleading if a given structure is not correctly described. This can be the case for systems with multireference character. In connection with pentalene, we note that DFT-based AI and HOMA values become unreliable in the case of the Jahn–Teller unstable D_{2h}-symmetrical form, which is a typical multireference system. The same holds for the D_{4h}-symmetrical cyclobutadiene or the D_{8h}-symmetrical planar cyclooctatetraene.

Another problem is the choice of the correct reference. Kekeule-benzene modeled by the properties of either *trans*- or *cis*-1,3-butadiene is a suitable reference for benzoide hydrocarbons as long as they are planar. Already in the case of the kekuléne, this is no longer given as the inner CH bonds move outside the carbon plane, which leads to small errors because the reference (Kekulé benzene) is planar. We have ignored this effect as it concerned just the CH bonds, but have refrained from applying the current approach to nonplanar conjugated π-systems such as the bridge [10]annulenes,[187] as they require different reference systems that absorb the strain and exchange effects so that the AI is still measuring the degree of π-delocalization rather than also other electronic effects. Strictly speaking, this applies also to polycyclic π-systems that contain three-, four-, five-, seven-, or eight-membered rings rather than just benzenoide conjugated rings. In each of these cases, the AI values have just a qualitative value as different reference systems have to be taken.

In this work, molecule **30** was used to test the influence of the chosen reference on results. Using the cyclohetatrienyl radical or *cis*-1,3-butadiene and the 1,4-pentadienyl radical in conformations determined by the equilibrium geometry of **30** leads to shift of the results obtained with Kekulé benzene as reference, i.e., ring E becomes more antiaromatic and the outer rings also antiaromatic. The analysis reveals that the use of references with more delocalized structures shift n_{opt} (R_{opt}) to a higher value and by this all HOMA values in the direction of more antiaromatic ones. Hence, the choice of a suitable reference is essential for any HOMA-based approach. In cases such as fulvene, this can be easily done by using as a reference molecule 2-vinyl-1,3-butadiene but excluding the 3,4-double bond from the bonds that determine n_{opt} (R_{opt}). Experience shows that results obtained in this way are close to results based on 1,3-butadiene itself. It is noteworthy that the approach described here can be based on a molecular form, which is characterized by one or more imaginary frequencies. The corresponding normal modes have to be projected out from the set of $3N - L$ modes, and then the local modes are determined from the remaining normal modes.

The AI provides a quantitative assessment of Clar's rule as is indicated in Figure 6, where we have also summarized the available heats of formation to facilitate stability comparisons. Clar's rule is only useful for single-string short benzoide hydrocarbons with not more than one benzene ring in the center. For longer strings such as the acenes, it fails to predict peripheral delocalization and the high-reactivity of the inner rings. It is also no longer useful for increasing degree of ring condensation as in the case of the circulenes, ovalene, or mixed ring systems such as **24** or **25**.

Similarly to cyclobutadiene and cyclooctatetraene, pentalene interconverts between C_{2h} isomers. In 1,3,5-tri-*tert*-butylpentalene the energy barrier was found to be 4 kcal/mol.[188] The calculated barrier height is 9.7 kcal/mol[189] and 6.6 kcal/mol (including ZPE).[190]

4. CONCLUSIONS

Based on the analysis presented in this work, the following conclusions can be drawn.

(1) The BSO values based on the local CC stretching force constants provide a more sensitive measure of π-delocalization than can be derived from CC bond lengths. The Badger rule[123,128] is not fulfilled, as the significant scattering of the k^a(CC) data points in Figure 3 reveals (R^2 = 0.937). Hence, any AI based on bond lengths is flawed because of the fact that bond lengths do not provide a reliable measure of the intrinsic bond strength.

(2) The HOMA is more sensitive with regard to the reference molecule used (*trans*- or *cis*-1,3-butadiene) than the AI value, which gives literally the same results for the two reference molecules. This has to do with the fact that α in eq 1 is much larger (282.9) compared to the γ (6.503) used in eq 4.

(3) However, it is equally true that anharmonicity corrections have a relatively large impact on the AI values in the way that aromaticity is slightly and antiaromaticity significantly reduced. Hence, in the harmonic approximation, only trends can be discussed, which may be considered as a disadvantage. However, this is outweighed by the fact that measured frequencies can be directly used to determine local stretching force constants and the corresponding AI values. Apart from this, there is always the possibility of scaling calculated harmonic frequencies or using, as done in this work, vibrational perturbation theory to get more reliable frequencies, close to measured values.

(4) The HOMA index exaggerates antiaromaticity by a factor of 1.5 and more, which becomes obvious for cyclobutadiene, pentalene, and all polycyclic systems containing the cyclobutadiene unit. Similarly exaggerated are differences in local aromaticities. We trace the difference between HOMA and the superior AI to the fact that the variation in the local CC stretching force constant is almost 7 mdyn/Å (corresponding to Δn(CC) = 1.25), whereas the bond lengths R(CC) vary by just 0.25 Å. Accordingly, a relative large constant α of 282.9 enters eq 1, whereas the value of γ in eq 4 is just 6.503 (harmonic

DOI: 10.1021/acs.joc.6b01761
J. Org. Chem. 2016, 81, 9669–9686

local modes) or 7.866 (anharmonic corrections included). In this way, any weakening/strengthening changes are largely exaggerated by the HOMA index as reflected by its more extreme values.

(5) BSO(CC) values larger than 1.19 (*trans*-1,3-butadiene as a reference) and smaller than 1.90 indicate some degree of cyclic π-delocalization. We define aromatic CC bonds as those with a BSO of 1.45 ± 0.25. This measure can be made more sensitive by determining local CCC bending force constants to quantify strain and steric effects (exchange repulsion) in general.

(6) The AIs of the ground and the S_1-excited state of the first acenes up to [5]acene have been determined to demonstrate that excitation leads to an inversion of aromatic delocalization so that in the S_1-state, the most inner ring is the least π-delocalized one, which explains the high reactivity of teracene and pentacene and their spontaneous dimerization under the influence of visible light. In the ground state, the acenes prefer a peripheral delocalization rather than the establishment of local aromatic units that dominate the stability.

(7) As has been found in many other investigations, Clar's rule ("the resonance structure with the most disjoint benzene units")[36,37,39] is surprisingly successful in predicting local aromaticity and thereby the most stable isomer of a molecule with different isomers. However, this is not always true. In the case of ovalene, the AI predicts a stable pyrene unit characterized by a central naphthalene-type 10π-system. The HOMA index is in line with Clar's rule suggesting four overlapping phenanthrene units leading to four benzene units (2 × A, 2 × D). Because of its lower sensitivity, the HOMA ignores the possibility of an inner 10π-delocalization that can also not be predicted on the basis of Clar's rule. Anharmonicity corrections confirm this trend.

(8) [4]-Phenancene **8** is 2.5 kcal/mol more stable than triphenylene, which is neither predicted by the AI nor the HOMA values, as the stability difference is a result of increased CH repulsion in three (**7**) rather than just two (**8**) bay regions. Peripheral π-delocalization is better in a phenancene such as **8**. Clar's rule fails to predict the correct ordering of stabilities, predicting **7** as the more stable system.

(9) Kekuléne is nonplanar and has D_{3d} rather than D_{6h} symmetry.[155] The symmetry lowering is due to the repulsion between the H atoms of the inner ring, which moves three H atoms upward and three downward. The HOMA values suggest that the outer 30π-delocalization is stronger than the inner 18π one, which is not correct. The AI gives the correct AI values (0.707 vs 0.598), suggesting that the inner π-delocalization is more aromatic than the outer one. Local 6π-aromaticity is preferred relative to peripheral 18π- (inner cycle) or 30π-aromaticity (outer cycle).

(10) AI and HOMA differ with regard to the description of coronene (**15**) and ovalene (**16**). According to the AI values, the highest local aromaticity should be in the central units of these π-systems, whereas HOMA predicts peripheral π-delocalization to be more pronounced.

(11) Cyclobutadiene is the prototype of an antiaromatic π-system, where the antiaromatic character is exaggerated by HOMA by a factor of 1.5−2 due to an exaggerated ALT (bond alternation) contribution. The necessity of correcting the AI value for anharmonic effects is given when a more reliable AI is needed. Local antiaromaticity is predicted by the AI values for **18**−**21**. The resulting destabilization is circumvented by forming nonaromatic π-systems (**18**; HOMA predicts antiaromaticity; **19** and **20**). This is not possible for **21**, which is antiaromatic according to both AI and HOMA values.

(12) Pentalene is the prototype of a bicyclic 8π antiaromatic system, which has an AI value of −0.190 (total; ring A: −0.215). It has to be emphasized that both the WS and the ALT values are exaggerated for four- and five-membered rings (thus leading to a more negative AI) because Kekulé benzene is not the appropriate reference. Nevertheless, the AI of pentalene is in line with an antiaromatic destabilization energy of −6.3 kcal/mol obtained for a *tert*-butyl derivative of pentalene.[147,148]

(13) The BSO values of the CH bonds of molecules **1**−**30** have been determined. The values reveal that the intrinsic strength of a CH bond is largely independent of the degree of π-delocalization in the corresponding ring. However, peri-CH bonds are always weakened, whereas CH bonds in bay regions are strengthened (from 1.012 in benzene to 1.024 in Kekuleńe, inner cycle) because of space confinement.

Future work will have to focus on the choice of suitable reference molecules besides Kekulé benzene that absorb strain and steric effects (exchange repulsion) in a way that also nonplanar conjugated π-systems can be systematically investigated. Also, a procedure to effectively scale harmonic frequencies to their measured counterparts by using local mode information has to be developed to fine-tune AI values close to those based on measured frequencies. In summary, the AI-concept developed in this work is broadly applicable and superior to the HOMA model.

■ ASSOCIATED CONTENT

Supporting Information

The Supporting Information is available free of charge on the ACS Publications website at DOI: 10.1021/acs.joc.6b01761.

Heats of formation for the molecules investigated in this work; CC and CH bond strength orders and interatomic distances for reference molecules; molecules containing the phenanthrene, pyrene, cyclobutadiene, fulvene, and heptafulvene unit. Correlation of relative bond strength orders and AIs; peripheral and individual AI values; peripheral and individual HOMA values. Harmonic approximation and anharmonicity corrections. Different references: *trans*- and *cis*-1,3-butadiene; comparison of HOMA and AI values; relative bond strength orders and anharmonicity corrections; HOMA values for (poly)-cyclic conjugated molecules. Cartesian coordinates of (poly)cyclic hydrocarbons investigated in this work (PDF)

■ AUTHOR INFORMATION

Corresponding Author

*E-mail: dieter.cremer@gmail.com.

Notes

The authors declare no competing financial interest.

DOI: 10.1021/acs.joc.6b01761
J. Org. Chem. 2016, 81, 9669−9686

■ ACKNOWLEDGMENTS

This work was financially supported by the National Science Foundation, Grants CHE 1464906 and CHE 1152357. We thank SMU for providing computational resources.

■ REFERENCES

(1) Minkin, V. I.; Glukhovtsev, M. N.; Simkin, B. Y. *Aromaticity and Antiaromaticity, Electronic and Structural Aspects*; Wiley: New York, 1994.
(2) Randic, M. *Chem. Rev.* **2003**, *103*, 3449−3605.
(3) Kertesz, M.; Choi, C. H.; Yang, S. *Chem. Rev.* **2005**, *105*, 3448−3481.
(4) Chen, Z.; Wannere, C. S.; Corminboeuf, C.; Puchta, R.; v. R. Schleyer, P. *Chem. Rev.* **2005**, *105*, 3842−3888.
(5) Mandado, M.; Moa, M. J. G.; Mosquera, R. A. *Aromaticity: Exploring Basic Chemical Concepts with the Quantum Theory of Atoms in Molecules*; Nova Science: New York, 2008.
(6) Gleiter, R.; Haberhauer, G. *Aromaticity and Other Conjugation Effects*; Wiley: New York, 2012.
(7) Krygowski, T. M.; Szatylowicz, H. *ChemTexts* **2015**, *1*, 1−12.
(8) Krygowski, T. M.; Bankiewicz, B.; Czarnocki, Z.; Palusiak, M. *Tetrahedron* **2015**, *71*, 4895−4908.
(9) Hückel, E. Z. *Eur. Phys. J. A* **1932**, *76*, 628−628.
(10) Hückel, E. *Grundzüge. der Theorie ungesättiger und aromatischer Verbindungen*; Verlag Chemie: Berlin, 1938.
(11) Krygowski, T. M.; Szatylowicz, H.; Stasyuk, O. A.; Dominikowska, J.; Palusiak, M. *Chem. Rev.* **2014**, *114*, 6383−6422.
(12) Feixas, F.; Matito, E.; Poater, J.; Sola, M. *Chem. Soc. Rev.* **2015**, *44*, 6434−6451.
(13) Gershoni-Poranne, R.; Stanger, A. *Chem. Soc. Rev.* **2015**, *44*, 6597−6615.
(14) Cocq, K.; Lepetit, C.; Maraval, V.; Chauvin, R. *Chem. Soc. Rev.* **2015**, *44*, 6535−6559.
(15) Szatylowicz, H.; Stasyuk, O. A.; Krygowski, T. M. *Adv. Heterocycl. Chem.* **2016**, *120*, 301−327.
(16) Fernandez, I.; Frenking, G.; Merino, G. *Chem. Soc. Rev.* **2015**, *44*, 6452−6463.
(17) Das, R.; Chakraborty, A.; Pan, S.; Chattaraj, P. K. *Curr. Org. Chem.* **2013**, *17*, 2831−2844.
(18) Paul, S.; Goswami, T.; Misra, A. *AIP Adv.* **2015**, *5*, 107211.
(19) Wheeler, S. E. *Acc. Chem. Res.* **2013**, *46*, 1029.
(20) Ramos-Berdullas, N.; Radenkovic, S.; Bultinck, P.; Mandado, M. *J. Phys. Chem. A* **2013**, *117*, 4679.
(21) Sokolov, A. Y.; Magers, D. B.; Wu, J. I.; Allen, W. D.; v. R. Schleyer, P., III; S, H. F. *J. Chem. Theory Comput.* **2013**, *9*, 4436.
(22) Stanger, A. *J. Org. Chem.* **2013**, *78*, 12374.
(23) Palusiak, M.; Domagala, M.; Dominikowska, J.; Bickelhaupt, F. M. *Phys. Chem. Chem. Phys.* **2014**, *16*, 4752.
(24) Pelloni, S.; Lazzeretti, P. *J. Phys. Chem. A* **2013**, *117*, 9083.
(25) Reisi-Vanani, A.; Rezaei, A. A. *J. Mol. Graphics Modell.* **2015**, *61*, 85−88.
(26) Pop, R.; Medeleanu, M.; van Staden, J.; Diudea, M. *Z. Phys. Chem.* **2016**, *230*, 285−296.
(27) Bauschlicher, C. W., Jr. *Chem. Phys.* **2015**, *448*, 43−52.
(28) Andjelkovic, L.; Gruden-Pavlovic, M.; Zlatar, M. *Chem. Phys.* **2015**, *460*, 64−74.
(29) Zborowski, K. K.; Alkorta, I.; Elguero, J. *Struct. Chem.* **2016**, *27*, 91−99.
(30) Dobrowolski, M. A.; Cyranski, M. K.; Wrobel, Z. *Phys. Chem. Chem. Phys.* **2016**, *18*, 11813−11820.
(31) Feixas, F.; Matito, E.; Poater, J.; Sola, M. *J. Comput. Chem.* **2008**, *29*, 1543−1554.
(32) Mercero, J. M.; Boldyrev, A. I.; Merino, G.; Ugalde, J. M. *Chem. Soc. Rev.* **2015**, *44*, 6519−6534.
(33) Feixas, F.; Jimenez-Halla, J. O. C.; Matito, E.; Poater, J.; Sola, M. *J. Chem. Theory Comput.* **2010**, *6*, 1118−1130.
(34) Heilbronner, E.; Bock, H. *The HMO Model and Its Application*; John Wiley & Sons: London, 1976; Vol. *1*: Basis and Manipulation.
(35) Zimmermann, H. E. *J. Am. Chem. Soc.* **1966**, *88*, 1564−1565.
(36) Clar, E. *The aromatic sextet*; John Wiley & Sons: London, 1972.
(37) Sola, M. *Front. Chem.* **2013**, *1*, 22.
(38) Das, R.; Chakraborty, A.; Pan, S.; Chattaraj, P. K. *Curr. Org. Chem.* **2013**, *17*, 2831−2844.
(39) Portella, G.; Poater, J.; Sola, M. *J. Phys. Org. Chem.* **2005**, *18*, 785−791.
(40) Nishina, N.; Makino, M.; Aihara, J. *J. Phys. Chem. A* **2016**, *120*, 2431−2442.
(41) Melendez-Perez, J. J.; Martinez-Mejia, M. J.; Eberlin, M. N. *Org. Geochem.* **2016**, *95*, 29−33.
(42) Chauvin, R.; Lepetit, C. *Phys. Chem. Chem. Phys.* **2013**, *15*, 3855−3860.
(43) Aihara, J. *Bull. Chem. Soc. Jpn.* **2008**, *81*, 241−247.
(44) Aihara, J. *Phys. Chem. Chem. Phys.* **2016**, *18*, 11847−11857.
(45) Abdukadir, A.; Kerim, A.; Tawar, T. *Chem. Phys. Lett.* **2016**, *643*, 47−52.
(46) Giambiagi, M.; de Giambiagi, M. S.; dos Santos Silva, C. D.; de Figueiredo, A. P. *Phys. Chem. Chem. Phys.* **2000**, *2*, 3381−3392.
(47) Bultinck, P.; Ponec, R.; Van Damme, S. *J. Phys. Org. Chem.* **2005**, *18*, 706−718.
(48) Bultinck, P.; Rafat, M.; Ponec, R.; van Gheluwe, B.; Carbo-Dorca, R.; Popelier, P. *J. Phys. Chem. A* **2006**, *110*, 7642−7648.
(49) Szczepanik, D. W.; Andrzejak, M.; Dyduch, K.; Zak, E.; Makowski, M.; Mazurb, G.; Mrozek, J. *Phys. Chem. Chem. Phys.* **2014**, *16*, 20514−20523.
(50) Cook, R.; Sumar, I.; Ayers, P. W.; Matta, C. F. *Electron Localization-Delocalization Matrices (LDMs): Theory and Applications*; Springer: Cham, Switzerland, 2016.
(51) Sumar, I.; Cook, R.; Ayers, P. W.; Matta, C. F. *Phys. Scr.* **2016**, *91*, 013001.
(52) George, P.; Trachtman, M.; Bock, C. W.; Brett, A. L. *J. Chem. Soc., Perkin Trans. 2* **1976**, *1976*, 1222−1227.
(53) Aihara, J. *J. Am. Chem. Soc.* **1995**, *117*, 4130−4136.
(54) Fernández, I.; Frenking, G. *Faraday Discuss.* **2007**, *135*, 403.
(55) Balaban, A. T.; Durevic, J.; Gutman, I.; Jeremic, S.; Radenkovic, S. *J. Phys. Chem. A* **2010**, *114*, 5870−5877.
(56) Aihara, J.; Makino, M.; Sakamoto, K. *J. Phys. Chem. A* **2013**, *117*, 10477.
(57) Badri, Z.; Foroutan-Nejad, C. *Phys. Chem. Chem. Phys.* **2016**, *18*, 11693−11699.
(58) Aihara, J.; Ishida, T.; Kanno, H. *Bull. Chem. Soc. Jpn.* **2007**, *80*, 1518−1521.
(59) Yu, J.; Sumathi, R.; Green, W. *J. Am. Chem. Soc.* **2004**, *126*, 12685−12700.
(60) Kruszewski, J.; Krygowski, T. *Tetrahedron Lett.* **1972**, *13*, 3839−3842.
(61) Krygowski, T. *J. Chem. Inf. Model.* **1993**, *33*, 70−78.
(62) Jug, K.; Koester, A. *J. Am. Chem. Soc.* **1990**, *112*, 6772−6777.
(63) Raczynska, E. D.; Hallman, M.; Kolczynska, K.; Stapniewski, T. M. *Symmetry* **2010**, *2*, 1485−1509.
(64) Frizzo, C. P.; Matrins, M. A. P. *Struct. Chem.* **2012**, *23*, 375−380.
(65) Cyranski, M. *Chem. Rev.* **2005**, *105*, 3773.
(66) Chen, Z.; Wannere, C. S.; Corminboeuf, C.; Puchta, R.; v. R. Schleyer, P. *Chem. Rev.* **2005**, *105*, 3842.
(67) Stanger, A. *J. Org. Chem.* **2006**, *71*, 883−893.
(68) Ucun, F.; Tokat, A. *Chem. Phys. Lett.* **2015**, *621*, 5−11.
(69) Poater, J.; Fradera, X.; Duran, M.; Solà, M. *Chem. - Eur. J.* **2003**, *9*, 400−406.
(70) Matito, E.; Duran, M.; Sola, M. *J. Chem. Phys.* **2005**, *122*, 014109.
(71) Araujo, D. M.; da Costa, T. F.; Firme, C. L. *J. Mol. Model.* **2015**, *21*, 248.
(72) Tokatlı, A.; Ucun, F. *J. Phys. Org. Chem.* **2014**, *27*, 380−386.
(73) Ostrowski, S.; Dobrowolski, J. C. *RSC Adv.* **2014**, *4*, 44158−44161.
(74) Dobrowolski, J. C.; Ostrowski, S. *RSC Adv.* **2015**, *5*, 9467−9471.
(75) Krygowski, T. M.; Cyranski, M. *Tetrahedron* **1996**, *52*, 10255−10264.

DOI: 10.1021/acs.joc.6b01761
J. Org. Chem. 2016, 81, 9669−9686

(76) Andrzejak, M.; Kubisiak, P.; Zborowski, K. K. *Struct. Chem.* **2013**, *24*, 1171−1184.
(77) Radenković, S.; Kojic, S. R. N. J.; Petronijevic, J.; Antic, M. *J. Phys. Chem. A* **2014**, *118*, 11591−11601.
(78) Raczynska, E. D.; Makowski, M.; Hallmanna, M.; Kaminska, B. *RSC Adv.* **2015**, *5*, 36587−36604.
(79) Sarigul, M.; Sari, A.; Kose, M.; McKee, V.; Elmastas, M.; Demirtas, I.; Kurtoglu, M. *Inorg. Chim. Acta* **2016**, *444*, 166−175.
(80) Dobrowolski, J. C.; Ostrowski, S. *RSC Adv.* **2015**, *5*, 9467−9471.
(81) Cremer, D.; Kraka, E. *Curr. Org. Chem.* **2010**, *14*, 1524−1560.
(82) Setiawan, D.; Kraka, E.; Cremer, D. *J. Phys. Chem. A* **2015**, *119*, 9541−9556.
(83) Kraka, E.; Setiawan, D.; Cremer, D. *J. Comput. Chem.* **2016**, *37*, 130−142.
(84) Kalescky, R.; Kraka, E.; Cremer, D. *Int. J. Quantum Chem.* **2014**, *114*, 1060−1072.
(85) Kalescky, R.; Zou, W.; Kraka, E.; Cremer, D. *J. Phys. Chem. A* **2014**, *118*, 1948−1963.
(86) Dauben, H. J., Jr.; Wilson, J. D.; Laity, J. L. *J. Am. Chem. Soc.* **1968**, *90*, 811.
(87) Gershoni-Poranne, R.; Stanger, A. *Chem. Soc. Rev.* **2015**, *44*, 6597−6615.
(88) Sundholm, D.; Fliegl, H.; Berger, R. J. *WIREs Comput. Mol. Sci.* **2016**, DOI: 10.1002/wcms.1270.
(89) Foroutan-Nejad, C. *Theor. Chem. Acc.* **2014**, *134*, 8.
(90) Cremer, D.; Günther, H. *Liebigs Ann. Chem.* **1972**, *763*, 87−108.
(91) Cremer, D.; Gräfenstein, J. *Phys. Chem. Chem. Phys.* **2007**, *9*, 2791−2816.
(92) Kraka, E.; Cremer, D. In *Chemical implication of local features of the electron density distribution in Theoretical Models of Chemical Bonding, the Concept of the Chemical Bond*; Maksić, Z., Ed.; Springer: Heidelberg, 1990; Vol. *2*; pp 453−542.
(93) Bader, R. F. W. *Atoms in Molecules, A Quantum Theory*; Oxford University Press: Oxford, 1990.
(94) Bader, R. F. W.; Slee, T. S.; Cremer, D.; Kraka, E. *J. Am. Chem. Soc.* **1983**, *105*, 5061−5068.
(95) Cremer, D.; Kraka, E.; Slee, T.; Bader, R.; Lau, C.; Nguyen-Dang, T.; MacDougall, P. *J. Am. Chem. Soc.* **1983**, *105*, 5069−5075.
(96) López, C. S.; Faza, O. N.; Cossío, F. P.; York, D. M.; de Lera, A. R. *Chem. - Eur. J.* **2005**, *11*, 1734.
(97) Griffiths, M. Z.; Popelier, P. L. A. *J. Chem. Inf. Model.* **2013**, *53*, 1714−1725.
(98) Gatti, C.; Cargnoni, F.; Bertini, L. *J. Comput. Chem.* **2003**, *24*, 422.
(99) Firouzi, R.; Ardani, S. S. *Phys. Chem. Chem. Phys.* **2014**, *16*, 11538−11548.
(100) Szczepanik, D. W. *Comput. Theor. Chem.* **2016**, *1080*, 33−37.
(101) Cremer, D.; Gauss, J. *J. Am. Chem. Soc.* **1986**, *108*, 7467−7477.
(102) Santos, J. C.; Andres, J.; Aizman, A.; Fuentealba, P. *J. Chem. Theory Comput.* **2005**, *1*, 83.
(103) Bultinick, P.; Ponec, R.; Gallegos, A.; Fias, S.; Van Damme, S.; Carbo-Dorca, R. *Croat. Chem. Acta* **2006**, *79*, 363−371.
(104) Sablon, N.; De Proft, F.; Solá, M.; Geerlings, P. *Phys. Chem. Chem. Phys.* **2012**, *14*, 3960−3967.
(105) Herges, R.; Geuenich, D. *J. Phys. Chem. A* **2001**, *105*, 3214.
(106) Otero, N.; Van Alsenoy, C.; Pouchan, C.; Karamanis, P. *J. Comput. Chem.* **2015**, *36*, 1831−1843.
(107) Ostojic, B. D.; Misic, S.; Dordevic, D. S. *Int. J. Quantum Chem.* **2013**, *113*, 1890−1898.
(108) Garcia-Borras, M.; Osuna, S.; Luis, J. M.; Swart, M.; Sola, M. *Chem. Soc. Rev.* **2014**, *43*, 5089−5105.
(109) Geerlings, P.; Fias, S.; Boisdenghien, Z.; De Proft, F. *Chem. Soc. Rev.* **2014**, *43*, 4989−5008.
(110) v. R. Schleyer, P.; Wu, J. I.; Cossio, F. P.; Fernandez, I. *Chem. Soc. Rev.* **2014**, *43*, 4909−4921.
(111) Fernandez, I.; Bickelhaupt, F. M.; Cossio, F. P. *Chem. - Eur. J.* **2014**, *20*, 10791−10801.
(112) Guo, Y.; Liu, Z.; Liu, H.; Zhang, F.; Yin, J. *Spectrochim. Acta, Part A* **2016**, *164*, 84−88.
(113) Murphy, V. L.; Reyes, A.; Kahr, B. *J. Am. Chem. Soc.* **2016**, *138*, 25−27.
(114) Mori, T.; Tanaka, T.; Higashino, T.; Yoshida, K.; Osuka, A. *J. Phys. Chem. A* **2016**, *120*, 4241−4248.
(115) Messersmith, R. E.; Tovar, J. D. *J. Phys. Org. Chem.* **2015**, *28*, 378−387.
(116) Sander, W. *Isr. J. Chem.* **2016**, *56*, 62−65.
(117) Kalescky, R.; Kraka, E.; Cremer, D. *J. Phys. Chem. A* **2014**, *118*, 223−237.
(118) Shimanouchi, T. *Tables of Molecular Vibrational Frequencies Consolidated*; National Bureau of Standards: Gaithersburg, MD, 1972; Vol. *I*.
(119) Linstrom, P.; Mallard, W. G. *J. Chem. Eng. Data* **2001**, *46*, 1059−1063.
(120) Konkoli, Z.; Cremer, D. *Int. J. Quantum Chem.* **1998**, *67*, 1−9.
(121) Wilson, E. B.; Decius, J. C.; Cross, P. C. *Molecular Vibrations. The Theory of Infrared and Raman Vibrational Spectra*; McGraw-Hill: New York, 1955.
(122) Cremer, D.; Larsson, J. A.; Kraka, E. In *Theoretical and Computational Chemistry, Vol. 5, Theoretical Organic Chemistry*; Parkanyi, C., Ed.; Elsevier: Amsterdam, 1998; pp 259−327.
(123) Kraka, E.; Larsson, J. A.; Cremer, D. In *Computational Spectroscopy: Methods, Ex- periments and Applications*; Grunenberg, J., Ed.; Wiley: New York, 2010; pp 105−149.
(124) Zou, W.; Kalescky, R.; Kraka, E.; Cremer, D. *J. Chem. Phys.* **2012**, *137*, 084114.
(125) Zou, W.; Kalescky, R.; Kraka, E.; Cremer, D. *J. Mol. Model.* **2012**, 1−13.
(126) Konkoli, Z.; Cremer, D. *Int. J. Quantum Chem.* **1998**, *67*, 29−40.
(127) Zou, W.; Cremer, D. *Chem. - Eur. J.* **2016**, *22*, 4087−4099.
(128) Badger, R. M. *J. Chem. Phys.* **1934**, *2*, 128−132.
(129) Kalescky, R.; Kraka, E.; Cremer, D. *J. Phys. Chem. A* **2013**, *117*, 8981−8995.
(130) Krygowski, T. M.; Cyranski, M. *Chem. Rev.* **2001**, *101*, 1385−1420.
(131) Kraka, E.; Cremer, D. *Rev. Proc. Quim.* **2012**, *118*, 39−42.
(132) Becke, A. D. *J. Chem. Phys.* **1993**, *98*, 5648−5652.
(133) Stephens, P. J.; Devlin, F. J.; Chablowski, C. F.; Frisch, M. J. *J. Phys. Chem.* **1994**, *98*, 11623−11627.
(134) Dunning, T. H. *J. Chem. Phys.* **1989**, *90*, 1007−1023.
(135) Chai, J.-D.; Head-Gordon, M. *Phys. Chem. Chem. Phys.* **2008**, *10*, 6615−6620.
(136) Chai, J.-D.; Head-Gordon, M. *J. Chem. Phys.* **2008**, *128*, 084106.
(137) Zhao, Y.; Truhlar, D. *Theor. Chem. Acc.* **2008**, *120*, 215.
(138) Lebedev, V. I.; Skorokhodov, L. *Russ. Acad. Sci. Dokl. Math.* **1992**, *45*, 587.
(139) Gräfenstein, J.; Cremer, D. *J. Chem. Phys.* **2007**, *127*, 164113.
(140) Barone, V. *J. Chem. Phys.* **2005**, *122*, 014108.
(141) Kjaergaard, H. G.; Garden, A. L.; Chaban, G. M.; Gerber, R. B.; Matthews, D. A.; Stanton, J. F. *J. Phys. Chem. A* **2008**, *112*, 4324.
(142) Kalescky, R.; Zou, W.; Kraka, E.; Cremer, D. *Chem. Phys. Lett.* **2012**, *554*, 243−247.
(143) Furche, F.; Ahlrichs, R. *J. Chem. Phys.* **2002**, *117*, 7433−7447.
(144) Casida, M.; Huix-Rotllant, M. *Annu. Rev. Phys. Chem.* **2012**, *63*, 287−323.
(145) Kraka, E.; Zou, W.; Filatov, M.; Gräfenstein, J.; Izotov, D.; Gauss, J.; He, Y.; Wu, A.; Polo, V.; Olsson, L.; Konkoli, Z.; He, Z.; Cremer, D. *COLOGNE16*; Southern Methodist University: Dallas, TX, 2016.
(146) Frisch, M. J.; Trucks, G. W.; Schlegel, H. B.; Scuseria, G. E.; Robb, M. A.; Cheeseman, J. R.; Scalmani, G.; Barone, V.; Mennucci, B.; Petersson, G. A.; Nakatsuji, H.; Caricato, M.; Li, X.; Hratchian, H. P.; Izmaylov, A. F.; Bloino, J.; Zheng, G.; Sonnenberg, J. L.; Hada, M.; Ehara, M.; Toyota, K.; Fukuda, R.; Hasegawa, J.; Ishida, M.; Nakajima, T.; Honda, Y.; Kitao, O.; Nakai, H.; Vreven, T.; Montgomery, J. A., Jr.; Peralta, J. E.; Ogliaro, F.; Bearpark, M.; Heyd, J. J.; Brothers, E.; Kudin, K. N.; Staroverov, V. N.; Kobayashi, R.; Normand, J.; Raghavachari, K.;

DOI: 10.1021/acs.joc.6b01761
J. Org. Chem. 2016, 81, 9669−9686

Rendell, A.; Burant, J. C.; Iyengar, S. S.; Tomasi, J.; Cossi, M.; Rega, N.; Millam, J. M.; Klene, M.; Knox, J. E.; Cross, J. B.; Bakken, V.; Adamo, C.; Jaramillo, J.; Gomperts, R.; Stratmann, R. E.; Yazyev, O.; Austin, A. J.; Cammi, R.; Pomelli, C.; Ochterski, J. W.; Martin, R. L.; Morokuma, K.; Zakrzewski, V. G.; Voth, G. A.; Salvador, P.; Dannenberg, J. J.; Dapprich, S.; Daniels, A. D.; Farkas, Ö.; Foresman, J. B.; Ortiz, J. V.; Cioslowski, J.; Fox, D. J. *Gaussian 09*, Revision C.01; Gaussian Inc.: Wallingford, CT, 2010.
(147) Roth, W.; Adamczaka, O.; Breuckmann, R.; Lennartz, H.-W.; Boese, R. *Chem. Ber.* **1991**, *124*, 2499−2521.
(148) Roth, W. R.; Klarner, F.-G.; Siepert, G.; Lennartz, H.-W. *Chem. Ber.* **1992**, *125*, 217−224.
(149) Portella, G.; Poater, J.; Bofill, J. M.; Alemany, P.; Solá, M. *J. Org. Chem.* **2005**, *70*, 2509−2521.
(150) Bouas-Laurent, H.; Dürr, H. *Pure Appl. Chem.* **2001**, *73*, 639−665.
(151) Schenck, G. O. *Naturwissenschaften* **1954**, *41*, 452−453.
(152) Cox, J. D.; Pilcher, G. *Thermochemistry of Organic and Organometallic Compounds*; Academic Press: New York, 1970.
(153) Nagano, Y.; Nakano, M. *J. Chem. Thermodyn.* **2003**, *35*, 1403−1412.
(154) Roux, M.; Temprado, M.; Chickos, J.; Nagano, Y. *J. Phys. Chem. Ref. Data* **2008**, *37*, 1855−1996.
(155) Jiao, H.; v. R. Schleyer, P. *Angew. Chem., Int. Ed. Engl.* **1996**, *35*, 2383−2386.
(156) Hirshfeld, F.; Rabinovich, D. *Acta Crystallogr.* **1965**, *19*, 235−241.
(157) Hirshfeld, F.; Rabinovich, D. *Acta Crystallogr.* **1995**, *B51*, 1036−10451.
(158) Wannere, K.; Sattelmeyer, C. S.; Schaefer, H. F., III; v. R. Schleyer, P. *Angew. Chem., Int. Ed.* **2004**, *43*, 4200−4206.
(159) Lungerich, D.; Nizovtsev, A. V.; Heinemann, F. W.; Hampel, F.; Meyer, K.; Majetich, G.; v. R. Schleyer, P.; Jux, N. *Chem. Commun.* **2016**, *52*, 4710−4713.
(160) Ivanov, A. S.; Boldyrev, A. I. *Org. Biomol. Chem.* **2014**, *12*, 6145−6150.
(161) Sondheimer, F.; Wolovsky, R.; Amiel, Y. *J. Am. Chem. Soc.* **1962**, *84*, 274−284.
(162) Cremer, D.; Kraka, E.; Joo, H.; Stearns, J. A.; Zwier, T. S. *Phys. Chem. Chem. Phys.* **2006**, *8*, 5304−5316.
(163) Wright, S. C.; Cooper, D. L.; Geratt, J.; Raimundi, M. *J. Phys. Chem.* **1992**, *96*, 7943−7952.
(164) Arnold, B. R.; Michl, J. *J. Phys. Chem.* **1993**, *97*, 13348−13354.
(165) Glukhovtsev, M. N.; Laiter, S.; Pross, A. *J. Phys. Chem.* **1995**, *99*, 6828−6831.
(166) Balci, M.; McKee, M. L.; v. R. Schleyer, P. *J. Phys. Chem. A* **2000**, *104*, 1246−1255.
(167) Sancho-Garcia, J. C.; Perez-Jimenez, A. J.; Moscardo, F. *Chem. Phys. Lett.* **2000**, *317*, 245−251.
(168) Maksic, Z. B.; Kovacevi, B.; Lesar, A. *Chem. Phys.* **2000**, *253*, 59−71.
(169) Mo, Y. R.; v. R. Schleyer, P. *Chem. - Eur. J.* **2006**, *12*, 2009−2020.
(170) Demel, O.; Pittner, J. *J. Chem. Phys.* **2006**, *124*, 144112.
(171) Karadakov, P. B. *J. Phys. Chem. A* **2008**, *112*, 7303−7309.
(172) Levchenko, S. V.; Krylov, A. I. *J. Chem. Phys.* **2004**, *120*, 175−185.
(173) Eckert-Maksic, M.; Vazdar, M.; Barbatti, M.; Lischka, H.; Maksic, Z. B. *J. Chem. Phys.* **2006**, *125*, 064310.
(174) Eckert-Maksic, M.; Lischka, H.; Maksic, Z. B.; Vazdar, M. *J. Phys. Chem. A* **2009**, *113*, 8351.
(175) Menke, J. L.; Patterson, E. V.; McMahon, R. J. *J. Phys. Chem. A* **2010**, *114*, 6431−6437.
(176) Zou, W.; Izotov, D.; Cremer, D. *J. Phys. Chem. A* **2011**, *115*, 8731−8742.
(177) Cremer, D.; Schmidt, T.; Bock, C. W. *J. Org. Chem.* **1985**, *50*, 2684−2688.
(178) Parkanyi, C.; Aaron, J.-J. In *Theoretical and Computational Chemistry, Vol. 5, Theoretical Organic Chemistry*; Parkanyi, C., Ed.; Elsevier: Amsterdam, 1998; pp 233−258.
(179) Stepien, B. T.; Cyranski, M. K.; Krygowski, T. M. *Chem. Phys. Lett.* **2001**, *350*, 537.
(180) Scott, L. T.; Hashemi, M. M.; Bratcher, M. S. *J. Am. Chem. Soc.* **1992**, *114*, 1920−1921.
(181) Scanlon, L.; Balbuena, P.; Zhang, Y.; Sandi, G.; Back, C.; Feld, W.; Mack, J.; Rottmayer, M.; Riepenhoff, J. *J. Phys. Chem. B* **2006**, *110*, 7688−7694.
(182) Anderson, A. G., Jr.; Stecker, B. M. *J. Am. Chem. Soc.* **1959**, *81*, 4941−4946.
(183) Bauder, A.; Keller, C.; Neuenschwander, M. *J. Mol. Spectrosc.* **1976**, *63*, 281−287.
(184) Yamamoto, K. *Pure Appl. Chem.* **1993**, *65*, 157−163.
(185) Hatanaka, M. *J. Phys. Chem. A* **2016**, *120*, 1074−1083.
(186) Acocella, A.; Havenith, R. W. A.; Steiner, E.; Fowler, P. W.; Jenneskens, L. W. *Chem. Phys. Lett.* **2002**, *363*, 64−72.
(187) Humason, A.; Zou, W.; Cremer, D. *J. Phys. Chem. A* **2015**, *119*, 1666−1682.
(188) Bischof, P.; Gleiter, R.; Hafner, K.; Knauer, K.; Spanget-Larsen, J.; Süss, H. *Chem. Ber.* **1978**, *111*, 932−938.
(189) Falchi, A.; Gellini, C.; Salvi, P.; Hafner, K. *J. Phys. Chem. A* **1998**, *102*, 5006−5012.
(190) Zywietz, T.; Jiao, H.; v. R. Schleyer, P.; de Meijere, A. *J. Org. Chem.* **1998**, *63*, 3417−3422.

DOI: 10.1021/acs.joc.6b01761
J. Org. Chem. 2016, 81, 9669−9686